Ultrasonics Sonochemistry 90 (2022) 106197

Contents lists available at ScienceDirect

Ultrasonics Sonochemistry

journal homepage: www.elsevier.com/locate/ultson

Enhancement of biogas production from individually or co-digested green algae *Cheatomorpha linum* using ultrasound and ozonation treated biochar

Ahmed El Nemr [a,*], Mohamed Aly Hassaan [a,*], Marwa Ramadan Elkatory [b], Safaa Ragab [a], Mohamed Ahmed El-Nemr [c], Luigi Tedone [d], Guisepe De Mastro [d], Antonio Pantaleo [d]

[a] National Institute of Oceanography and Fisheries (NIOF), Marine Pollution Department, Environment Division, Alexandria 21556, Egypt
[b] Advanced Technology and New Materials Research Institute, City for Scientific Research and Technological Applications, Alexandria 21934, Egypt
[c] Department of Chemical Engineering, Faculty of Engineering, Minia University, Minia 61519, Egypt
[d] Bari University, Department of Agriculture and Environmental Sciences, Bari 70121, Italy

ARTICLE INFO

Keywords:
Biogas
Anaerobic digestion
Macroalgae
Sawdust Biochar
Sonication
Ozonation

ABSTRACT

This paper proposes the use of modified biochar, derived from Sawdust (SD) biomass using sonication (SSDB) and Ozonation (OSDB) processes, as an additive for biogas production from green algae *Cheatomorpha linum* (*C. linum*) either individually or co-digested with natural diet for rotifer culture (*S. parkel*). Brunauer-Emmett-Teller (BET), Fourier-Transform Infrared (FTIR), thermal-gravimetric (TGA), and X-ray diffraction (XRD) analyses were used to characterize the generated biochar. Ultrasound (US) specific energy, dose, intensity and dissolved ozone (O_3) concentration were also calculated. FTIR analyses proved the capability of US and ozonation treatment of biochar to enhance the biogas production process. The kinetic model proposed fits successfully with the data of the experimental work and the modified Gompertz models that had the maximum R^2 value of 0.993 for 150 mg/L of OSDB. The results of this work confirmed the significant impact of US and ozonation processes on the use of biochar as an additive in biogas production. The highest biogas outputs 1059 mL/g VS and 1054 mL/g VS) were achieved when 50 mg of SSDB and 150 mg of OSDB were added to *C. linum* co-digested with *S. parkle*.

1. Introduction

AD (anaerobic digestion) is a well-known and established technology, which often is affected by process instability, mainly when utilized with refractory feedstock [1,2]. Two of the most significant difficulties in AD are the low methane production yield and process inhibition due to detrimental inhibitor accumulation [3]. On the other side, biochar is often employed as a soil amendment; however, its retention of nutrients and its microbial development properties make it an attractive supplement for boosting anaerobic digestion processes [4]. Biochar's morphology and porous structure may cause bacteria immobilisation, resulting in increased digestion and methane production [2,5].

Additionally, biochar's conductive characteristics facilitate direct inter-species electron transfer (DIET), increasing methane synthesis [6–8]. Several investigations have demonstrated that biochar can reduce the time required to produce methane. Additionally, it was discovered that a high surface area of biochar facilitates biofilms' production and the sequestering of CO_2. Biochar can have either a helpful or a harmful influence on the anaerobic digestion process because the difference in feedstock and pyrolysis conditions of biochar production have different effects on its physicochemical characterizations [9]. As an electron acceptor, oxidized biochar facilitates ethanol production from volatile fatty acids (VFA). The reduced form of biochar, on the other hand, contributes to nitrate reduction through its role as an electron donor. It also benefits by buffering the inhibitory effects of moderate ammonia toxicity and other damaging inhibitors, enhancing the pace at which microbes reproduce [3,9,10].

Chen et al. [11] reported on the grinding method for preparing biochar nanoparticles, whereas Wang et al. [12] reported on the US method for preparing biochar nanoparticles. In general, it is believed that US and grinding are two excellent methods for simulating the natural weathering of biochar [13].

The ash component of biochar comprises minerals included in the original biomass, typically insoluble calcium and magnesium

* Corresponding authors.
E-mail addresses: ahmedmoustafaelnemr@yahoo.com (A. El Nemr), mhss95@mail.com (M.A. Hassaan), luigi.tedone@uniba.it (L. Tedone), giuseppe.demastro@uniba.it (G. De Mastro), antonio.pantaleo@uniba.it (A. Pantaleo).

https://doi.org/10.1016/j.ultsonch.2022.106197
Received 5 August 2022; Received in revised form 29 September 2022; Accepted 9 October 2022
Available online 11 October 2022

carbonates, and is a byproduct of the carbonization process. Carbon dioxide sequestration activity and alkalinity of biochar are enhanced due to the presence of these minerals, which help reduce the quantity of carbon dioxide emitted into the atmosphere. Biochar has a high carbon dioxide sequestration activity and is naturally alkaline, making it an excellent carbon dioxide sequestration material. This is referred to as mineral carbonation, and it occurs when calcium and magnesium-containing minerals react with carbon dioxide to generate stable carbonates, providing a safe and permanent storage solution for carbon dioxide [9,14,15].

An additional study investigating the role of biochar as a buffering agent discovered that biochar improved the buffering system during the anaerobic digestion of chicken manure and kitchen waste, significantly increasing the amount of biogas produced and the amount of methane released [3]. It was also discovered that biochar formed from fruit forests increased methane production by 47 percent and reduced the lag phase by 23 percent during anaerobic digestion of granular sludge using fruit forest anaerobic digestion.

However, it was discovered that coarse and medium-sized biochar granules favored methanogenesis, but small biochar particles favored fermentation and acidogenesis [8]. Small biochar particles, on the other hand, favored fermentation and acidogenesis. Adding biochar granules in the range of 0.5–1.0 mm in size to a crop can reduce the lag phase by 11 percent while simultaneously increasing the rate of methane synthesis by 86 percent, according to a study on the effects of fruitwood-generated biochar on crop growth. Anaerobic digestion was explored in this study by examining the impact of different types of biochar. The data demonstrate the need to use the correct amount of biochar during the entire digestion process, which was carried out in this study. According to one study, there has been some evidence that applying excessive biochar has a deleterious effect on methanogenesis.

As early as the first decade of the twenty-first century, research on biochar made from maize straw, coconut shells, and municipal solid waste demonstrated that biochar-supplemented setups produced less methane daily [16]. On the other hand, biochar made from coconut shells and corn straws showed a gradual rise in methane production after acclimation [16]. They reported that adding unmodified biochar at concentrations of 50 and 100 mg to algae significantly increased their biogas production compared to the same amount of algae that had not been treated [16–18]. Using 100 mg of unmodified biochar combined with 10 mg of Fe_2O_3 in the inoculum, it was revealed that a maximal amount of biogas (219.5 mL/g VS) was formed, and the highest amount of biogas generation was achieved. After experimenting with several combinations of biochar and Fe_2O_3, it was revealed that inoculating the inoculum with 100 mg of unmodified biochar mixed with 10 mg of Fe_2O_3 yielded the highest amount of biogas generation.

Biochar that has been sonicated and ozonated has been used exclusively for this study to test its effect on biogas production from green algae *C. Linum*, alone or in conjunction with *S. parkle* (S. parkle® is a ready-to-use dry diet for rotifers. This diet offers a performing and cost-effective product that allows – as the name suggests a sparkling clean rotifer production. It is formulated with high-quality, protected ingredients and manufactured following INVE Aquaculture's renowned strict quality control process). By comparing the performance of sawdust biochar containing NH_4OH (SD-NH_2), which was made from sawdust biomass, with that of unmodified (SD) and modified (SD-NH_2) biochar, we hope to enhance biogas generation from the red algae *Pterocladia capillacea* even further. As part of our research, we are looking into different methods of treating biochar that is utilized as an additive manufacturing of biogas. In the author's knowledge, this analysis is among the first researches to assess the effect of US and ozonation on the biochar individually or co-digestion (Co) with other dietary for the biogas production from algae *C. Linum*.

2. Materials and methods

2.1. Collection of green algae C. linum

To manufacture the final product, *C. linum*, a green alga, was harvested from the Mediterranean Sea off the coast of Alexandria in Egypt and gently treated with water to remove contaminants before being rinsed multiple times with distilled water and dried in an oven to produce the final product. It was necessary to treat and crush the dry algae to a particle size of around 0.5 mm before storing it until it was required for further usage. It has been computed that the amount of dry matter follows the literature [17,18]. The ash concentration of powdered dried samples was determined by ashing them for 24 h in a muffle furnace set to 550 °C. Carbon and nitrogen concentrations were evaluated using a CHN analyzer.

2.2. Synthesis of biochar

Sawdust (SD) is the precursor used to create biochar, and it was obtained from a local Egyptian market. After that, they are rinsed multiple times with tap water. It was necessary to dry the cleaned sawdust at a temperature of 105 °C before the dried SD could be milled and crushed further. In a refluxed system (200 °C), a soxhlet was used to boil the crushed SD in a 1000 mL solution of 75 % H_2SO_4 for 2 h. After that, the samples were filtered and washed with distilled water until the washing solution was neutralized [19,20].

2.3. US pretreatment

In a 100-mL distilled water solution of SDB, the produced neutral solution was sonicated for 30 min. The precipitated SDB was filtered, washed several times with distilled water, and then washed once with ethanol, followed by oven-dried at 105°for 24 h before being used. SSDB was the product's code designation. The pretreatment of biochar in the United States was carried out using a sonicator (QSonica 700). We employed a maximum power of 700 W (99 percent amplitude) and a fixed working frequency of 20 kHz for this experiment [22,23]. The Pyrex glass beakers (100 mL) were filled with the US tip. After undergoing US pretreatment, the specific energy, US dose, US density, and US intensity were all measured. All pretreatment studies in the US were repeated, and the final results were reported as mean values. The specific input energy (SE) of sludge solids is defined as the amount of energy given per unit mass of solids in the sludge. The following equation (1) describes the strength of the object [24]:

$$SE = \frac{P \times t}{TS \times V} \tag{1}$$

where SE (kJ/kg TS) = Specific energy in P = US power in kW, t = US time in second (s).

US dose: the US dose is the energy amount supplied per unit of sludge volume (equation (2)) [25]:

$$US\ dose = \frac{P \times t}{V} \tag{2}$$

US density: the US density is the power supplied per unit of biochar volume (equation (3)):

$$US\ density = \frac{P}{V} \tag{3}$$

US intensity (I): The US intensity (W/cm^2), (I) is proportional to the probe size and reflects the power delivered through the tip probe area. It may be computed using the following equation (4) [26]:

$$US\ Intensity = \frac{P \times t}{A} \tag{4}$$

where P = US power in kW, V = Volume of US sludge in liters (l), TS =

Table 1
The composition of the *S. parkle*.

Typical composition	
Crude lipids	12 %
Crude protein	38.9 %
Crude ash	5 %
Phosphorus	0.8 %
Crude Fibre	0.5 %
Vitamin A	500000 IU/kg
Ca	0.1 %
Vitamin D3	50000 IU/kg
Na	0.1 %
Vitamin E	3600 IU/kg
DHA	8.5 mg/g dwt
Vitamin C	4000 mg/kg
EPA	4.5 mg/g dwt
ARA	0.6 mg/g dwt

Table 2
A review of the substrates and pretreatment techniques used in batch tests to estimate the biogas production.

Experiment batch	Pretreatment
B-1	Manure + algae untreated (control)
B-2	Manure + algae + SSDB 50 mg/L
B-3	Manure + algae + SSDB 100 mg/L
B-4	Manure + algae + SSDB 150 mg/L
B-5	Manure + algae + OSDB 50 mg/L
B-6	Manure + algae + OSDB 100 mg/L
B-7	Manure + algae + OSDB 150 mg/L
B-8	Manure + algae untreated + *S. parkle* (Co-control)
B-9	Manure + algae + *S. parkle* + Co- SSDB 50 mg/L
B-10	Manure + algae + *S. parkle* + Co- SSDB 100 mg/L
B-11	Manure + algae + *S. parkle* + Co- SSDB 150 mg/L
B-12	Manure + algae + *S. parkle* + Co- OSDB 50 mg/L
B-13	Manure + algae + *S. parkle* + Co- OSDB 100 mg/L
B-14	Manure + algae + *S. parkle* + Co- OSDB 150 mg/L

Total solid concentration in g/l, t = US time in second (s), and A = Surface area in cm^2.

2.4. Preparation of ozonized biochar (OSDB)

As previously described [27,28], O_3 was created using an O_3 generator and connected through silicone tubing to a glass diffuser, where the prepared SDB was ozonized for 30 min in distilled water. The mixture was filtered and washed with distilled water and once with ethanol before being oven-dried overnight at 105 °C and designated as OSDB. It was decided to employ the KI titration method reported by Eaton et al. [29] to evaluate the O_3 content in the sample's gaseous and liquid phases. It has been reported that these procedures have been used in several water treatment plants and that they are applicable across the entire O_3 concentration range reported by Rakness and colleagues [30]. The system's detection limit depends on the system, and these iodometric titrations are cost-effective and apply to both phases [31]. O_3 gas is formed following the passage of O_3 gas through a solution containing a specified amount of potassium iodide at a steady flow rate. In the presence of sodium thiosulphate ($Na_2S_2O_3$), any of the products will react to generate a pale yellow solution, as can be seen in the photo. Do a titration after each addition of the starch solution until the blue color is totally eliminated. All experiments were carried out a total of three times to ensure accuracy. At the end of the process, the O_3 concentration is calculated with the help of the following equation (5):

$$O_3 \text{ concentration } (mg/L) = \frac{24 \times Vt \times Nt}{V} \quad (5)$$

where V is the bubble volume, V_t is the volume of $Na_2S_2O_3$ utilized (in milliliters), and N_t is the normality of the $Na_2S_2O_3$ solution.

2.5. Biochar pH determination

The pH of biochar was tested in three replicates ($n = 3$) using 1.0 g of biochar and Millipore water (10 mL) in each conical flask [32]. The results showed that biochar has a pH of 7. To ensure that the biochar slurry was thoroughly mixed, it was shaken for one hour at 100 rpm per minute using the JSOS-500 shaker. Using a JENCO pH metre, Model 6173, after each sample had been shaken, the pH of each sample was determined.

2.6. Source of S. parkle

S. parkle is a Batch diet for a consistent, performing rotifer culture. The powder was obtained from National Institute of oceanography and fisheries, Alexandria Branch and (Table 1) contains all the compositions of the used powder.

2.7. Measurement and characterization

The following approaches were used to characterize the SSDB, and OSDB biochar samples: FTIR analysis was made in the wavenumber range (400–4000 cm^{-1}) using VERTEX70 spectroscopy connected to ATR platinum model V-100 manufactured in Germany. X-ray samples were analyzed using Bruker Meas Srv (D2-208219)/D2-2082019 XRD equipment manufactured in Germany operating at 30 kV, 10 mA, with a Cu tube (λ = 1.54 Å) using a range from 5 to 100°. BET analysis was performed using Mini II, BEL Japan equipment, Inc., Osaka, Japan. Thermal studies were done on both manufactured biochars using the SDT650-Simultaneous Thermal Analayzer equipment in the range of 50 to 900 °C using a 5 °C per minute ramping temperature [18].

2.8. Creating the inoculum and substances

Cow dung was acquired from a slaughterhouse in the Egyptian city of Alexandria. The faeces were removed from the cage and placed in a black plastic garbage bag to be disposed of properly. Once it had cooled, it was placed in a plastic box container until it was needed the following morning. Before use, the cow poo was diluted one-to-one (w/v) with water to ensure it was ready to use.

2.9. Biogas tests

The digester configuration consisted of three bottles: a 100 mL digesting bottle, a 1000 mL water displacement bottle, and a water collection bottle. The digester configuration was designed to be mobile. The digester configuration was designed to be portable. The digester system has previously been successfully tested [33]. The containers were connected with plastic tubing, and the volume of gas created was determined by measuring the amount of water that was displaced by the containers. It was necessary to insert a piece of silicon plastic between the cap and the gas outflow port to ensure that the digester was entirely sealed against infiltration. Two-minutes flushing with pure nitrogen before the experiment was performed to eliminate oxygen from the system and convert it to anaerobic conditions. The amount of biogas produced was calculated by measuring the water displaced. Various concentrations of SSDB biochar and OSDB biochar were blended with *C. linum*, either alone or in combination with *S. parkle*, to investigate the effects of the additions on AD performance and biogas production yield. All treatments were carried out at 37°Celsius for 70 days. The batch AD experiments were carried out in triplicate, and the results were reported as an average of the three studies' results. The substrates that were utilized in batch studies to evaluate biogas output are given in the following table (Table 2).

Table 3
Approximate values for the various substrates are provided.

Tests of Proximate	*C. linum*	Manure
TS%	86.15	8.04
Ash%	27.63	15.30
VS%	72.37	84.70
C%	23.38	48.92
N%	2.47	4.21
H%	4.65	5.45
S%	4.079	–
C/N	9.46	11.64

2.10. An investigation of the mechanics of production and statistical analysis

To estimate cumulative biogas production, many studies have employed nonlinear regression models (such as the modified Gompertz model), logistic functions, and first-order models (such as equations 6–8) [34–36]. The correlation coefficient (R^2) was calculated to compare the accuracy of the studied models using the Excel 2010 and Origin 2020b techniques, respectively.

$$M = Pb \times exp\left\{ -exp\left[\frac{Rm \times e}{Pb}(\lambda - t) + 1\right]\right\} \quad (6)$$

$$M = \frac{Pb}{\left(1 + exp\left\{\frac{4Rm}{Pb}(\lambda - t) + 2\right\}\right)} \quad (7)$$

$$M = Pb(1 - exp[-kt]) \quad (8)$$

where M (L/g VS added) shows the yield of biogas per time t (days), Pb (L/g VS added) shows the substrate's maximum potential of biogas, k denotes the rate constant of hydrolysis (1/day), t (day) shows the time, Rm (L/g VS added) shows the maximum production rate of biogas, λ is the lag time of phase (days), e (2.7183) is Euler's function constant.

3. Results and discussion

3.1. Physiochemical properties of pretreated biochar

3.1.1. Chemical compositions of C. linum

The VS content of *C. linum* is 72.37 % and a C/N ratio was 9.46 (Table 3). The majority of literature [18] recommends a working C/N ratio of between 20 and 30 with an ideal ratio of 25 for anaerobic bacterial growth in the AD system, which is still significantly lower than the measured ratio for *C. linum*.

3.1.2. Fourier Transform Infrared spectrum (FTIR)

The FTIR spectrum (Fig. 1) is consistent with those of previous biochars generated via chemical treatment (sulfonation), followed by pretreatment with US and O_3 [19–21,37,38]. Peak at 783.4 cm^{-1} indicates the presence of alkene compounds and C═C bending. Additionally, it implies a higher concentration of benzene derivatives or aromatic chemicals in SDB than in SSDB or OSDB. The presence of aromatic esters between 1203.44 and 1380 cm^{-1} is indicated by peaks between 1203.44 and 1380 cm^{-1}. Due to the presence of alcohols, bands between 1035 cm^{-1} indicate silica and C—O. The peaks at 1479.2 and 1600 cm^{-1} exhibit C═C bending, consistent with various aromatic ring modes and alkenes [39,40]. The strong peak at 1027 cm^{-1} indicates that OSDB stretches CO with more intensity than SDB and SSDB. The peaks 1380–1496 cm^{-1} belong by O—H stretching, which correlates to carboxylic acid. During the ozonation process, the strength of the O—H stretching vibration band grew significantly more than that of SDB and SSDB. The peaks between 3259 and 3378 cm^{-1} are represented to O—H. The strength of the O—H stretching vibration band decreased much more than it did for SDB and OSDB and shifted somewhat to the lower zone of frequency, which indicates a decrease in the amount of OH groups. There is no specific difference between biochar from different treatments, which can be attributed to the fact that the change that occurs due to the various treatments is physical and not chemical.

3.1.3. X-ray diffraction (XRD) and elemental analysis

Amorphous carbon structure C (002) with randomly aligned aromatic sheets is indicated by the diffraction peaks for SDB, SSDB, and OSDB (Fig. 2), which are broad diffraction peaks in the range 2Θ =

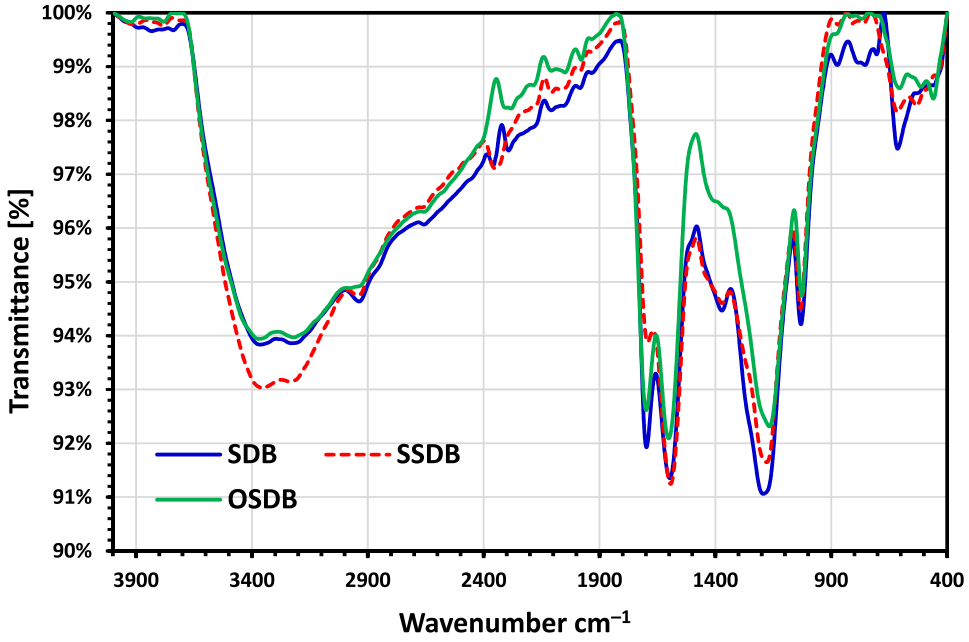

Fig. 1. FTIR analysis of SDB, SSDB and OSDB.

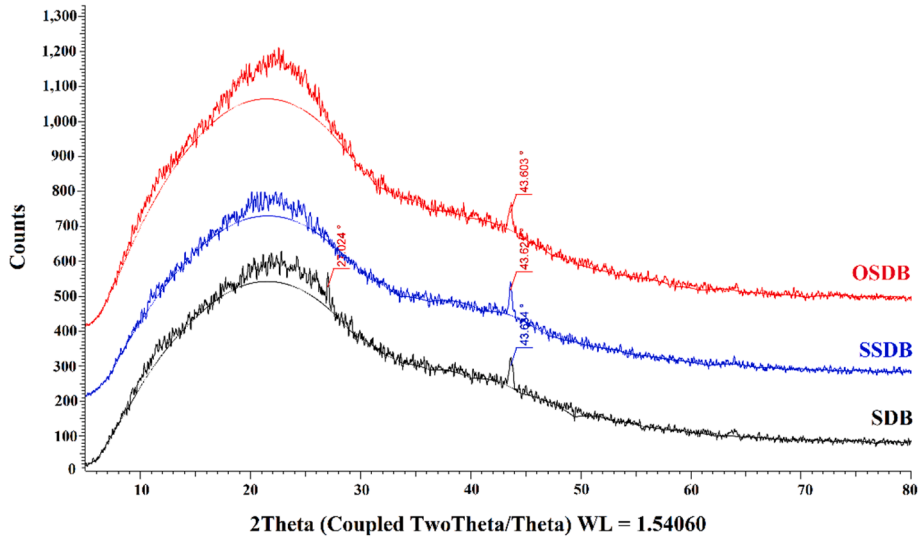

Fig. 2. XRD analysis of SDB, SSDB and OSDB.

Table 4
The percentage of the elemental contents to determine chemical composition of untreated and pretreated biochar.

Material	Elements content (%)		
	C	H	O
SDB	77.4	9.7	12.9
SSDB	78	12.5	9.5
OSDB	71.6	4.5	23.9

10–30°. There are sharp peaks in the vicinity of $2\Theta = 27$ and 43.65°. In the case of OSDB, sharp peaks around 2Θ = 25.8, 43.6, and 63.9°correspond to various inorganic components, primarily composed of quartz, albite, and/or calcite, within the structure of SDB, indicating that the original feedstock was high in Si, as indicated by the Si-O-Si stretching band in the FTIR spectrum. As the pyrolysis temperature rises, the crystallinity of mineral components increases, resulting in highly structured aromatic structures in the SDB, SSDB, and OSDB biochars [41]. Elemental analysis determines the biochar's bulk composition and is valuable for determining the degree of change caused by US and O_3 treatments. As demonstrated in (Table 4), there is a slight change due to US and O_3 treatments. The findings revealed that sonolysis could result in hydrogenation (the fixation of hydrogen from water) and reductive fixation of carbon (from dissolved CO_2). Such findings are amplified when CO_2-saturated water is used (which is not the case here), as the carbon content increased from 77.4 percent of the untreated sample to 78 percent of the 30-minute US-treated sample. However, the carbon content of the untreated sample decreases significantly from 77.4 percent to 71.6 % after 30 min of O_3 treatment. Additionally, there appears to be an increase in the oxygen content in the biochar samples, from 12.9 percent for the untreated biochar to 23.9 percent for the 30-minute O_3-treated biochar sample.

3.1.4. *Thermal analysis (TGA)*

The SDB is decomposed in three steps, whereas the SSDB and OSDB are decomposed in 2 steps (Fig. 3). The first phase occurred between 50 and 150 °C as a consequence of the loss of surface-bound water and moisture in the sample, resulting in a weight loss of 6.7 and 13.21 percent for SDB and SSDB, respectively. This is followed by the second stage, which results in weight loss of 56.30 percent at 150–350 °C, 22.55 percent at 350–1,000 °C and 30.03 percent at 275 °C–1000 °C (SDB and

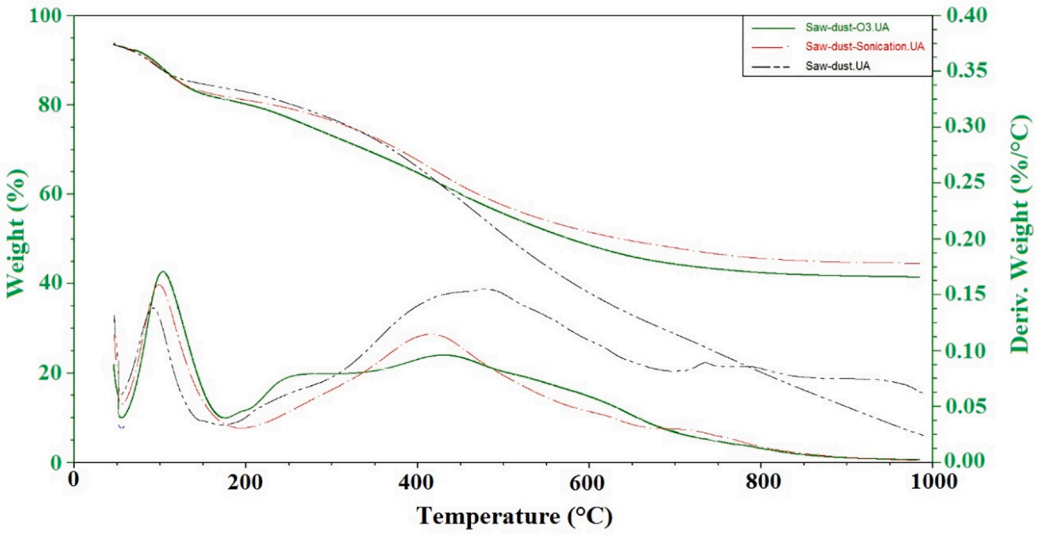

Fig. 3. TGA analysis of SDB, SSDB and OSDB.

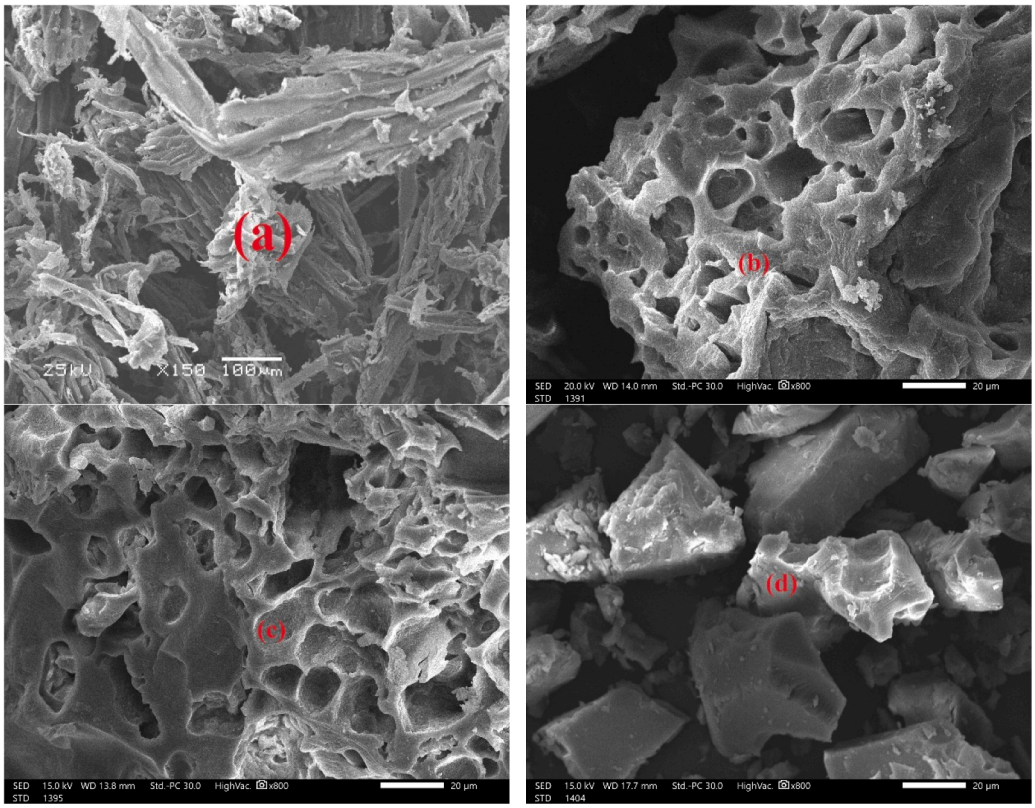

Fig. 4. SEM image of (a) raw SD, (b) SDB, (c) SSDB, and (d) OSDB.

Table 5
Biochar surface area and porosity as measured by BET.

Sample of biochar	S_{BET} (m^2/g)	r_p (nm)	V_p (cm^3/g)
SDB	2. 913	16.824	0.0122
SSDB	4.009	14.728	0.01476
OSDB	1.974	10. 716	0.00529

SSDB), respectively. The weight remained of SSDB and the percentages of 2.96 % obtained and the curves of DTA reflect more stability for SSDB, and OSDB treated with US and O_3 sample than SDB; this refers increases susceptibility to consuming them during digestion by anaerobic bacteria, which explain that the cumulative biogas production was high in case of using SSDB and OSDB biochar than SDB [20,21].

3.1.5. Scanning electron microscopy (SEM)

These SEM images (Fig. 4) indicate that raw biochar had a non-smooth surface and many small particles, and its pores were observed of different sizes due to the loss of volatile matter [17]. After acoustic activation, acidic activation (H_2SO_4) combined with Sulphur functionalization increased mesoporous and micro-porous. The surface of the carbon material was smooth compared to biochar, with no pretreatment. As opposed to amorphous silicon, the surface of SSDB was more porous and comprised several opening pores, most of which had no content in their pore channels. As a result of the US reaching the under-layers and breaking down the biochar structure, pores were formed on the top layer and between the layers, resulting in interlayer pores. The material's surface got cleaner, more micro- and meso-pores formed, and micro- and meso-channels formed. SEM analysis demonstrates that the US treatment improves porosity and dissociates weakly linked components of the biochar surface (for example, labile carbon (LC) and volatile matter (VM)). The OSDB, on the other hand, exhibits collapsed porosity, indicating the physical changes to the biochar surface caused by ozonation pretreatment.

The SDB, SSDB, and OSDB characteristics are listed in (Table 5), together with the specific surface area (S_{BET}, m^2/g), total pore volume (V_p, cm^3/g), and mean pore diameter (r_p, nm). The surface area of biochars increased from (SDB) 2.913 to (SSDB) 4.009 m^2/g by treating biochar with US due to increasing different pore sizes; the mean pore diameters decreased from SDB 16.824 to SSDB 14.728 nm (mesopores), respectively, total pore volume slightly increased from (SDB) 0.0122 to (SSDB) 0.01476 cm^3/g. These results revealed that the modification process reduces the r_p of SSDB. While, the S_{BET}, r_p, and V_p of OSDB are decreased to 1. 974 m^2/g, 10. 716 nm and 0.00529 cm^3/g, respectively, when the biochar was treated with O_3. Results showed that after chemical treatment of biochar, the surface area, mean pore diameters, and total pore volume reduced due to SDB broken into small pieces with a lower surface area and pore blockage induced by the new functional groups developing on the surface of the material.

3.2. Impact of biochar on the production of biogas

3.2.1. Impact of biochar modifications on the production of biogas

The methane generation yields over time are shown in Fig. 5. The laboratory work findings of biogas output yields were gathered over 70 days, and the results are depicted in (Fig. 6). As illustrated in (Fig. 6), when the *C. linum* was treated with an SSDB at doses of (100, 50 mg/L), and an OSDB at a dose of (150 mg/L), the average production yield of biogas was increased marginally when compared to the average production yield of biogas when the *C. linum* was not treated with biochar. It was discovered that when *C. linum* was treated with 50 mg Co-SSDB, a significant favorable effect on biogas generation (p 0.05) was found. The 50 mg and 150 mg/L dosages of Co-SSDB and Co-OSDB, respectively, produced the highest biogas yield with 1059 and 1054 mL/g VS for *C. linum* co-digested with *S. Parkle*. Additionally, when *C. Linum* was individually treated with OSDB at concentrations of 50, 100, and 150 mg/L, the production yield of biogas was raised more than the production yield of biogas from the control sample, yielding 536, 600, and

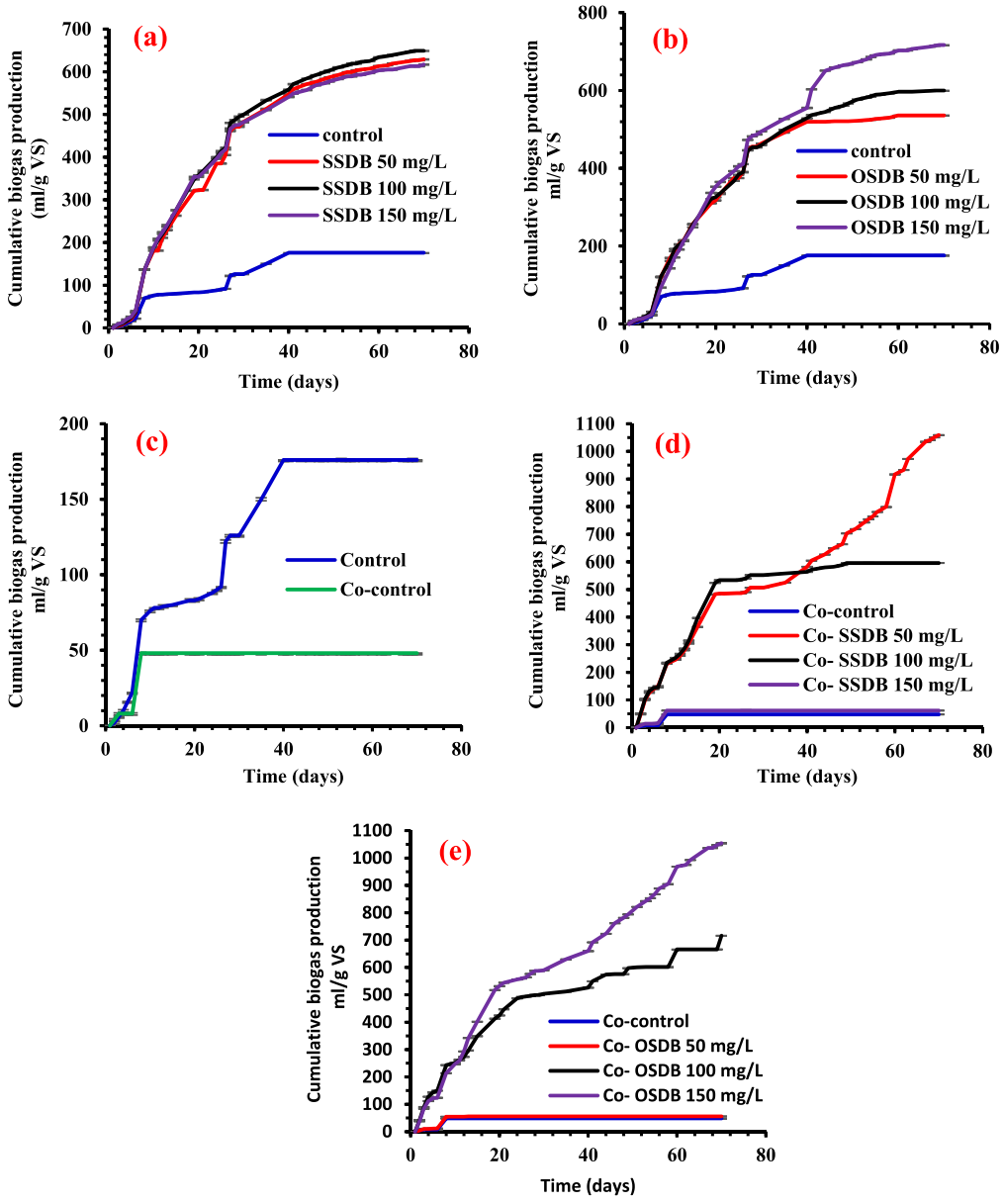

Fig. 5. Production of cumulative net biogas (mL/g VS) on an average basis employing (a) SSDB, (b) OSDB, (c) Control and Co-control, (d) Co-SSDB, and (e) Co-OSDB.

717 mL/g VS respectively. The same enhancement happened when *C. linum* was treated with SSDB with different dosages (50, 100, and 150 mg/L), which produced a higher biogas yield (629, 649, and 617 mL/g VS), respectively.

(Fig. 6) shows that most groups' daily biogas production yield exhibited several peaks, with the occurrence time and persistence period of the peaks varying from one group to the other. Several months after the final biogas production apex, gas output in all 14 groups gradually decreased, signaling the conclusion of AD. Methanogens were able to produce their maximal biogas output within the first 0–10 days of digestion in all digesters, which may be due to the presence of dissolved and easily degradable chemicals in the feedstock. Volatile organic acids (VFAs) are also formed gradually during the hydrolysis of soluble organic compounds. In contrast, when the accumulation of VFAs exceeded the regulating capability of biochar, the methanogenic activity of methanogens was suppressed, resulting in a significant reduction in biogas production rate. Hassaan et al. [17] also showed that the greater intermediate product concentrations inhibited the AD process.

When *C. linum* was digested alone or in combination with *S. parkle* and treated with SSDB, the development of the second peak of the biogas occurred earlier than in the control and co-control treatment groups. If prepared biochar and co-additives (such as *S. parkle*) contain alkaline groups on their surfaces, this may be due to the fact that they can neutralize vast amounts of organic acids produced during the early stages of AD, thereby alleviating the acid inhibition phenomena that occur within the system. Second, SSDB has a higher specific surface area than SDB, making it ideal for the metabolism and growth of methanogens and other microorganisms. In contrast, OSDB has a lower specific surface area than SDB but contains more functional groups, making it an excellent choice for methanogen metabolism and growth. Finally, the effectiveness of SSDB and OSDB is enhanced when algae are co-digested with *S. parkles*. Possibly because *S. parkles* has nutrients that methanogens can utilize to boost their activity and the effectiveness of VFA conversion, the plant's efficacy may be attributed to the fact that it feeds nutrients to methanogens. Immediately following the second peak, daily methane production began to decline rapidly in lockstep with the degradability of organic matter, as shown in the graph (Fig. 6).

The biogas production rate recovered significantly from day 24 to 70

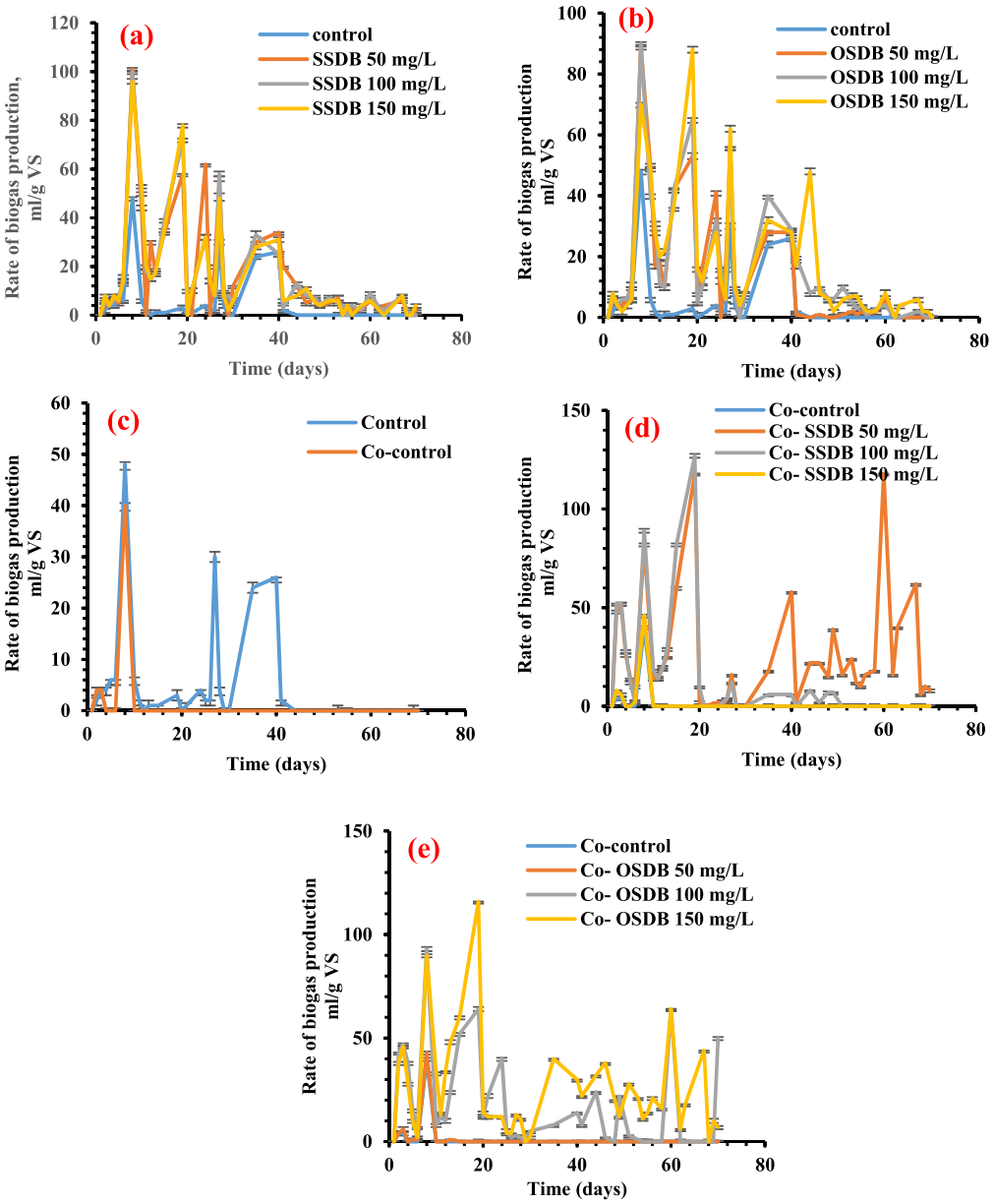

Fig. 6. Production of cumulative net biogas (mL/g VS) on an average basis employing (a) SSDB, (b) OSDB, (c) Control and Co-control, (d) Co-SSDB, and (e) Co-OSDB.

for all treatments, demonstrating that methanogens consume and digest organic compounds that may be difficult to degrade to produce methane in the AD system. As the number of chemicals available to methanogens decreases, biogas generation gradually increases, and the AD process concludes after 70 days. This phenomenon was primarily caused by the physical properties of biochars, which are highly dependent on the feedstock, pyrolysis conditions, and physical modification to alter the surface structure via the addition of additional active sites via the US or chemical alteration via ozonation. To avoid ammonia toxicity, the Co process attempts to balance the algae's comparatively high nitrogen content with another high carbon substrate by adjusting digestion variables such as duration of residence, reactor design, loading rates, and the temperature of digestion [17]. Following a brief time of adaption and reproduction, methanogens gradually adjust to their environment and rapidly enhance biogas generation. While Co-control produces poor yield biogas due to ammonia accumulation caused by algae in the digester, which inhibits microbial activity if it exceeds the encouraged methanogen growth rate. The cumulative production yields of biogas for the several test groups are depicted in Fig. 5. The results demonstrated that various pretreatments of biochar using US, O_3 procedures, and co-additives for previously described pretreated biochar had varying beneficial effects on methane and biogas production. When *C. Linum* is co-digested with *S. Parkle* treated with 50 mg/L of SSDB, the maximum biogas yield increases by 501.7 percent compared to when *C. Linum* is treated alone. Clearly, the biochar characterization is influenced by the type of pretreatment of biochar and co-additives (*S. parkle*). Additionally, previous research has indicated that aromatization, porosity generated by US and O_3 processes, and co-additive (*S. parkle*) biochar may all affect biochar's effect on AD.

3.2.2. *Biochar dosage effect on biogas production*

Experiments demonstrated that various types of biochar treated with US and O_3 accelerated biogas generation significantly. Apart from the type of biochar used, the dose of biochar can also affect biogas yield. As a result, the influence of biochar doses on the cumulative biogas yield was examined, and the results are depicted in Fig. 5. Compared to the Control group, the incremental yield % of biogas is increased by 501.7, 498.8, 307.3, 306.8, 268.7, 257.3, 250.5, 204.5, and 249.4 % when the

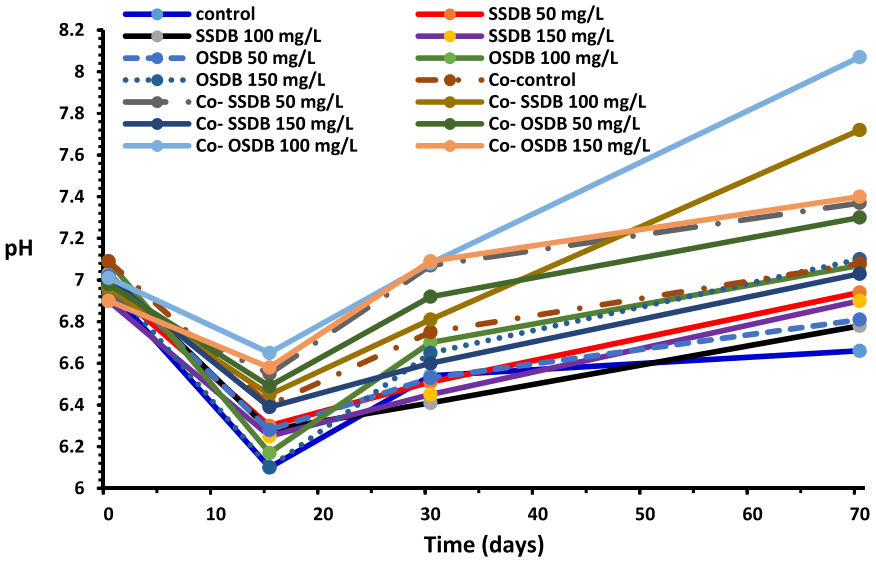

Fig. 7. Variation of pH during AD of different substrates.

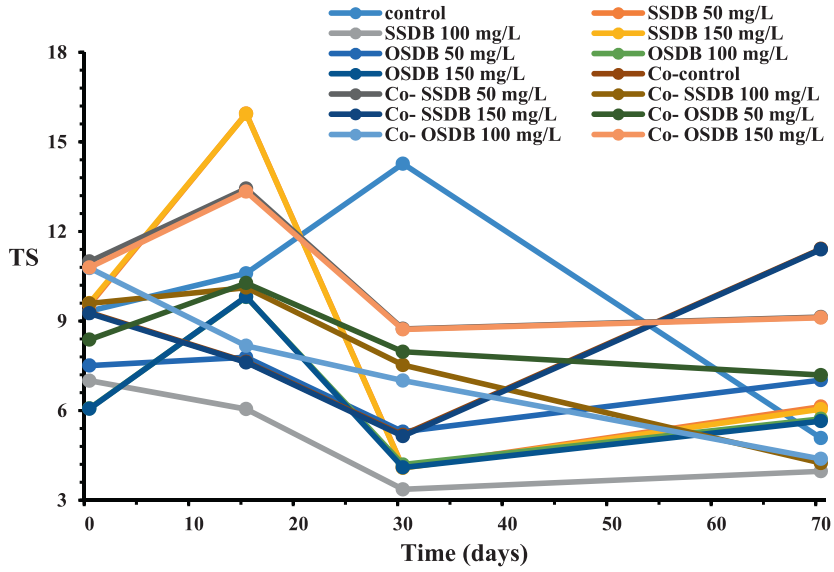

Fig. 8. Variation of TS during AD of different substrates.

Co-SSDB (50), Co-OSDB (150), OSDB (150), Co-OSDB (100), SSDB (100), SSDB (50), SSDB (150), OSDB (50), and OSDB (100 mg/L) were added, respectively. However, increasing the amount of SSDB to 150 mg/L resulted in a significant decrease in the cumulative yield percent of biogas, which was 64.7 percent less than that of the control group treated with 0 mg/L biochar (Fig. 5c). The results demonstrated that when biochar was added at a higher concentration, it had a clear inhibitory impact, decreasing biogas yield. For Co-SSDB, the most significant cumulative biogas yield occurred at a dose of 50 mg/L (1059 mL/g VS), while a significant decrease in yield was observed when Co-SSDB was administered at a dose of 150 mg/L (Fig. 5d). When Torri [10] carried out a similar investigation in which he added corn-derived biochar to an AD system, he discovered that biochar's addition enhanced the cumulative methane emission, but it also increased the rate at which the reaction took place. A further discovery was indicated that the best amount of biochar to use was 10.0 g L^{-1}, and that increasing the amount resulted in a drop in methane emissions. Because moderate biochar addition effectively mitigated VFA accumulation and resulted in increased methanogenic activity [24], whereas a higher biochar concentration resulted in increased propionic acid accumulation and lowered the stability of the AD process [25], the authors concluded that moderate biochar addition was the most effective option for their research. Moreover, according to a study by Lü et al. [8], methane output increased by 23.5–47.1 percent in digesters containing biochar compared to controls that did not include biochar [17–21]. Total methane outputs compared to the control group increased by 12.07 percent, 21.19, 33.65, and 45.66 percent in the biochar treatment groups. Additionally, three to six increasing peaks in daily biogas yield were tested, both with and without the inclusion of biochar treatment. It was discovered that adding biochar to the mix could lead daily biogas outputs to peak substantially earlier than in the control study [17–21]. For example, Co-SSDB 50 mg/L demonstrated six peaks in daily biogas yields on the 3rd, 8th, 19th, 40th, 60th, and 67th days of fermentation, whereas the control group demonstrated peaks on the 8th, 27th, and 41st days (Fig. 5d). Aside from the fact that it is extremely biodegradable, biochar can supply sustenance to methanogens throughout the

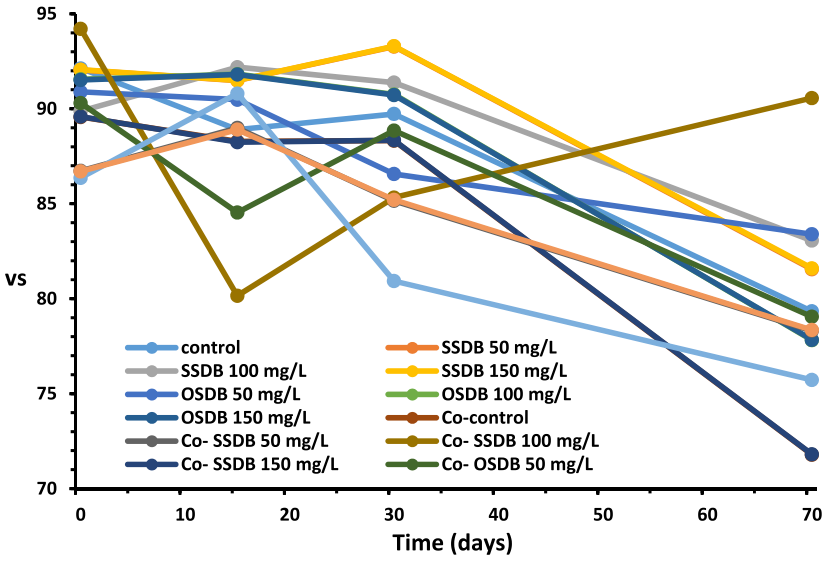

Fig. 9. Variation of VS during AD of different substrates.

Table 6
Results of different parameters of the US and ozonation.

Measurements	Values
US power	500 W
Frequency	20 KHZ
US time in second	1800 S
Specific input energy	92.934 kJ/kg TS
US dose	9000 kJ/L
US density	5 kW/L
Probe Surface area	418 cm^2
US Intensity	177.87 W/cm^2
O_3 time in second	1800 S
O_3 production per hour	500 (mg/hr)
O_3 dose	1.1 mg/L
Dissolved O_3 concentration	0.85 mg/L
pH of US biochar	3.91 + 0.28
pH of O_3 biochar	1.86 + 0.25

Table 7
Kinetic analysis data using a modified Gompertz model.

	R^2	Predicted P (ml/g VS)	Differences (%)	Rmax mL/g VS.day	ƛ (day)
SSDB					
control	0.946	187.33 + 6	3.9	14.52 + 0.98	0.07 + 0.01
50 SSDB	0.991	622.22 + 6.71	1.9	14.58 + 0.34	0.09
100 SSDB	0.991	637.52 + 6.53	2.4	14.07 + 0.33	0.09
150 SSDB	0.991	603.18 + 5.97	2.7	13.33 + 0.32	0.09 + 0.04
OSDB					
control	0.946	187.33 + 6	3.9	14.52 + 0.98	0.07 + 0.01
50 OSDB	0.992	535.46 + 4.59	0.32	12.87 + 0.28	0.11
100 OSDB	0.992	599.37 + 5.91	0.83	14.40 + 0.31	0.09
150 OSDB	0.993	722.51 + 8.10	0.85	16.93	0.08
Co-SSDB					
Co-Control	0.976	48 + 0.39	0	6.05	12.30
50 Co-SSDB	0.946	1646.68 + 355.08	4.9	38.49 + 10.56	0.02
100 Co-SSDB	0.987	593.54 + 4.69	0.43	8.26 + 0.24	0.14
150 Co-SSDB	0.949	62.20 + 0.70	0.32	5.92 + 0.16	0.92 + 0.19
Co-OSDB					
Co-Control	0.976	48 + 0.39	0	6.05	12.30
50 Co-OSDB	0.970	55.92 + 0.50	0.15	6.19 + 0.15	2.25 + 1.61
100 Co-OSDB	0.972	638.31 + 10.28	11.5	10.08 + 0.53	0.08
150 Co-OSDB	0.965	1085.76 + 49.89	6.2	18.49 + 1.41	0.05

digestion process, increasing microbial activity and methane production in the environment.

It was discovered that Co resulted in a synergistic effect in which the amount of methane produced exceeded the amount expected by each co-solo substrate's digestion in a previous experiment [42,43]. This method is based on the concept that when ordinary algal biomass is digested, it creates chemicals that hinder the digestive process, primarily ammonia. Reduced ammonia nitrogen concentrations can be achieved by combining algae with low-cost, high-carbon wastes, which may minimize ammonia inhibitor levels in the water. Yen and Brune [44] discovered that waste paper co-digesting with algae results in a C:N ratio of 20:1–25:1 for methane production, which is similar to the optimal C:N ratio for other substrate. In addition to raising the methane yield by 50 % over that obtained by algae digestion alone, adding paper to the digester increased the methane yield by another 50 %. They also theorized that adding paper to the mix boosted cellulose activity, assisting in breaking algal cell walls. In our study, the Co substrates were biochar and *S. parkle*. Additionally, biochar has been shown to be an effective adsorbent of indirect inhibitors or contaminants such as antibiotic residues [45], oily substances [46], pesticides [47], metal ions [48] and metal ions [16] dispersed in water, and as a reactant in the biochars labile carbon methanization process [49]. When biogas and biochar are combined in a system, they can benefit from several profitable synergies that can improve digestive quality by facilitating direct interspecies electron transfer, promoting microbial immobilisation and metabolism, increasing fertilizer nutrient retention, and lowering the inhibition and accumulation of interspecific products [16,49,50].

As part of the first stage, US is used to induce microjets through the surface of the biochar, which penetrates through the surface of the biochar, exfoliating and fracturing the irregularly shaped biochar to change its surface area and pore distribution while simultaneously lowering its mineral content. The anaerobic digestion of algae was

Table 8
Kinetic data analysis utilizing the Logistic model.

	R^2	Predicted P (ml/g VS)	Differences (%)	Rmax mL/g VS.day	ʎ (day)
SSDB					
control	0.945	181.87 + 4.69	2.6	20.48 + 1.09	0.10 + 0.01
50 SSDB	0.982	607.69 + 7.37	3.5	19.14 + 0.50	0.13 + 0.01
100 SSDB	0.980	623.79 + 8.05	3.9	18.68 + 0.51	0.14 + 0.01
150 SSDB	0.979	592.09 + 7.62	4.1	17.83 + 0.51	0.14 + 0.01
OSDB					
control	0.945	181.87 + 4.69	2.6	20.48 + 1.09	0.10 + 0.01
50 OSDB	0.984	528.76 + 5.79	1.4	17.05 + 0.42	0.16 + 0.01
100 OSDB	0.982	586.17 + 7.30	2.4	19.07 + 0.49	0.13 + 0.01
150 OSDB	0.984	698.17 + 9.42	2.9	21.85 + 0.54	0.12 + 0.01
Co- SSDB					
Co-Control	0.977	48.07 + 0.38	0.14	6.63 + 0.16	2.03 + 0.42
50 Co-SSDB	0.937	1407.18 + 0.23613	3.8	46.47 + 9.17	0.04 + 0.01
100 Co-SSDB	0.988	587.11 + 4.32	1.5	11.40 + 0.26	0.20 + 0.01
150 Co-SSDB	0.964	62.24 + 0.59	0.39	6.28 + 0.18	0.91 + 0.12
Co- OSDB					
Co-Control	0.977	48.07 + 0.38	0.14	6.63 + 0.16	2.03 + 0.42
50 Co-OSDB	0.976	56.05 + 0.45	0.1	6.53 + 0.14	1.31 + 0.18
100 Co-OSDB	0.958	624.08 + 10.46	12.9	14.78 + 0.71	0.12 + 0.01
150 Co-OSDB	0.949	1024.02 + 42.86	7.1	25.66 + 1.89	0.07 + 0.001

Table 9
Kinetic data analysis utilizing a first-order model.

	R^2	Predicted P (ml/g VS)	Differences (%)	K (1/day)
SSDB				
control	0.949	211.87 + 10.61	6.8	0.031 + 0.01
50 SSDB	0.978	743.23 + 26.03	3.9	0.030 + 0.01
100 SSDB	0.979	751.79 + 23.79	3.5	0.031 + 0.01
150 SSDB	0.979	659.19 + 19.54	2.9	0.034 + 0.01
OSDB				
control	0.949	211.87 + 10.61	6.8	0.031 + 0.01
50 OSDB	0.964	604.09 + 19.66	5.4	0.039 + 0.03
100 OSDB	0.979	711.96 + 24.02	5.1	0.031 + 0.01
150 OSDB	0.979	961.38 + 50.50	5.8	0.022 + 0.01
Co- SSDB				
Co-Control	0.817	49.20 + 1.30	2.5	0.134 + 0.02
50 Co-SSDB	0.950	1548.88 + 209.87	8.7	0.014 + 0.01
100 Co-SSDB	0.969	616.24 + 9.49	2.5	0.068 + 0.01
150 Co-SSDB*	–	–	11.4	–
Co- OSDB				
Co-Control	0.817	49.20 + 1.30	2.5	0.134 + 0.02
50 Co-OSDB	0.836	57.35 + 1.41	2.4	0.135 + 0.02
100 Co-OSDB	0.985	677.44 + 10.21	9	0.05 + 0.01
150 Co-OSDB	0.982	1308.12 + 63.72	4.5	0.02 + 0.01

*Faild.

improved due to the development of redox-active organic functional groups on the surface of biochar following the application of O_3 to the material (Fig. 1). It was found that the characteristic peak in FTIR at 1400 cm^{-1} (OH and C—H) in OSDB was more evident than the corresponding peak in SSDB and SDB (Fig. 1), resulting in superior anaerobic digestion of untreated algal performance over SSDB and SDB (Table 1). As a result, the most likely explanation for these observations was that biochar facilitated interspecies electron transfer by functioning as an electron mediator or shuttle rather than an electron conduit, as previously suggested.

S. parkle is another potential co-substrate for algae digestion, but it was found that depending on the adaptation procedure, mixed bacterial populations can lose their ability to degrade a protein substrate [51], with the yield of biogas dropping from 176 to 48 mL/g VS when *S. parkle* was added to untreated algae. Protein and lipids are the principal elements of *S. parkle*, with the latter, due to its high energy content, playing the most essential role in AD for the production of biogas [52]. Protein is the most essential component of *S. parkle's* composition. Lipids are long-chain fatty acids (LCFAs) linked to glycerol, alcohols, or other groups by using ester or ether bonds. Lipids are found in various foods, including meat, fish, and poultry. Lipids can be found in a number of plant and animal tissues, as well as in the blood. During hydrolysis, lipids are rapidly broken down into monomers such as glycerol LCFAs, and these monomers are then converted into short organic acids through oxidative degradation [53]. Short organic acids are transformed into acetate and hydrogen due to this conversion, which are then converted into methane and carbon dioxide [52]. Compared to biogas produced from carbs and proteins, biogas produced from lipids contains much more significant methane quantities [53]. A high organic loading or LCFAs prevented the production of biogas from lipid even though the gas quality was improved [54,55]. High organic loading or LCFAs also stopped the production of biogas from lipid despite the improved quality of the gas. According to Koster and Cramer's research work [56], LCFAs have been demonstrated to inhibit several activities during the AD process. Concentrations as low as 50 mg/L of LCFAs have been shown to have inhibitory effects on the growth of bacteria [57]. Additionally, LCFAs have a considerable inhibitory effect on AD bacteria, particularly methanogens and acetogens [57]. Methanogens grow slowly and are particularly sensitive when exposed to the harsh circumstances of the procedure. As a result, methanogens require more time to be retained in digesters [52]. anti-methanogen chemicals are also effective against methanogens. To produce a high methane output, the optimal carbon/nitrogen/phosphorus (C/N/P) ratio is approximately 100:3:1 [58–60], and the *S. parkle* has 389 percent protein. Anaerobic fermentation is characterized by differences in the physiological characteristics of acidogens and methanogens and differences in food requirements, growth kinetics, and environmental sensitivity [58]. The failure to maintain equilibrium between these two groups is the most fundamental source of process instability [59]. Because of the increased danger of ammonia inhibition [61], it is not recommended to employ large amounts of energy-dense [60] proteinaceous substrate in the AD process. As suggested by the literature [58], the inhibitory level of total ammonia concentration varies depending on variables such as the inoculum, the substrate, and the amount of acclimation required, the length of the operation, the pH, and the temperature of the environment. The explanation is that free NH_3 is membrane permeable [59] and causes a proton imbalance and a potassium shortage, making it the most prevalent source of inhibitory action. Although a decreased biogas yield has been observed when *S. parkle* is used, this has been attributed to an increased ammonia load. The feeding of the substrate with high nitrogen content in conjunction with a significant number of carbon-rich

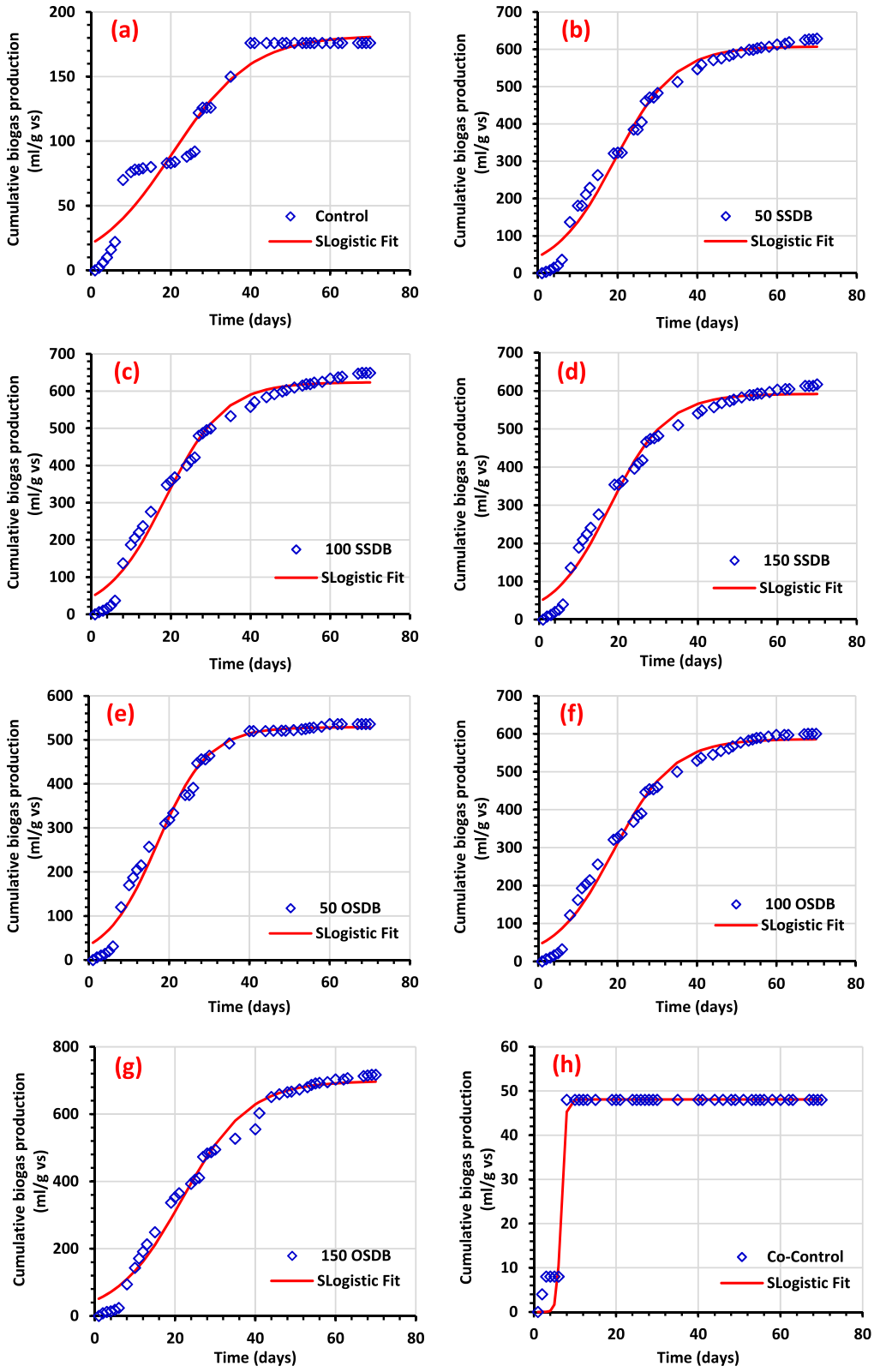

Fig. 10. Cumulative biogas yield from Logistic model, (a) Control (b-d) SSDB, (e-g) OSDB, (h) Co-Control (i-k) Co-SSDB and (L-n) Co-OSDB.

materials has been attempted to reach the requisite C/N/P ratio but has proven unsuccessful.

S. parkle's digestibility can be increased by mixing them with high-carbon substrates, which improves the C/N ratio. This could result in considerable improvements in the pore properties of biochar due to the biochar responsible for boosting C/N ratio and removing NH_3 through pores created on the surface of pretreatment biochar by US and O_3 treatments. Given that functional groups on biochar surfaces such as

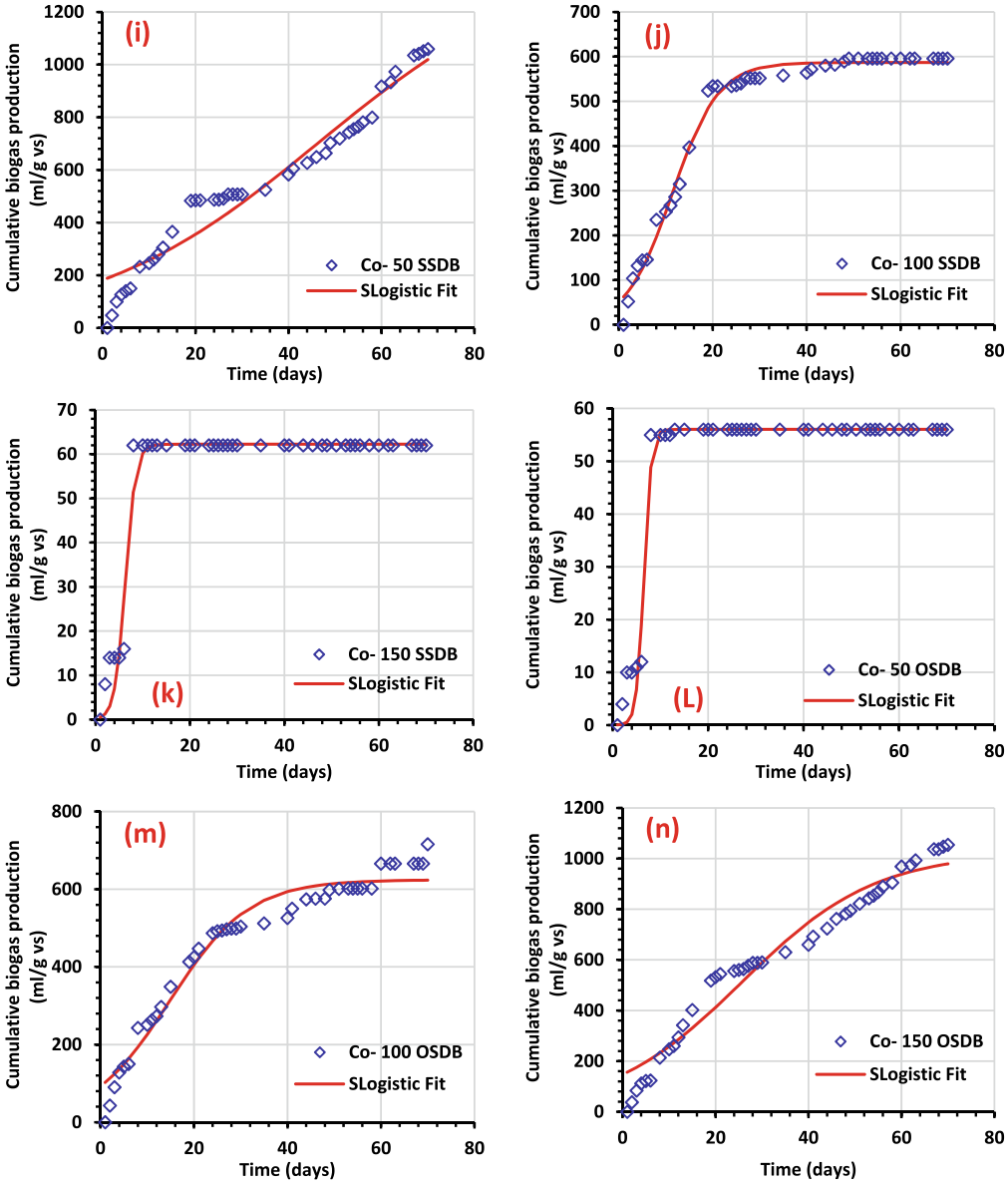

Fig. 10. (*continued*).

COOH and phenolic groups (which have a net negative surface charge) can interact directly with multi-valence cations to produce organo-mineral complexes [62]. These are likely oxygen-containing groups triggered these reactions on biochar surfaces. As a result of its high sorption capacity for gaseous NH_3 and aqueous ammonium ions, biochar that has been synthesized with US and O_3 has been shown to lower ammonium emissions from *N*-rich S. parkle plants by as much as 50 % [63]. The most excellent biogas yields in SSDB with 50 mg/L and OSSDB with 150 mg/L, respectively, were 1059–1054. The results show that pretreatment biochar with US and O_3 removes inhibitors from the reaction medium throughout the AD process, improves the C/N ratio, and stabilizes anaerobic bacteria for biogas production.

The influence of biochar on the fermentation process was evident in the change in pH during AD. According to previous research, the optimal pH range for the growth of AD bacteria is 6.6–7.6 [64–66]. pH is a crucial parameter for tracking the progression of Alzheimer's disease and influencing microbial activity and metabolic pathways. Because of the alkaline nature of biochar, pH values in digesters with biochar addition increased, as expected (Fig. 7). Overall, it appeared that the pH of all groups decreased during the first 10 days of AD, which was most likely due to the accumulation of VFAs generated by the breakdown of organics in the slurry [67], which was most likely due to the accumulation of VFAs generated by the breakdown of organics in the slurry [68]. The pH of the control group decreased from 6.96 to 6.1, but the lowering was limited in the biochar treatment digesters due to the organic alkali functional groups in the biochar [68]. The ingestion of VFAs and the ammonification of protein, in addition to the aforementioned causes, led in a rise of the pH value in all digesters, which was observed in all digesters. The pH of biochar-amended digesters was slightly alkaline (6.9–8.03), considerably higher than the control group (6.9–7.08). At a pH lower than 6.6, methanogenic activity was severely suppressed in the digesters without biochar addition (untreated algae with manure and Co of untreated algae with *S. parkle* and faeces), resulting in a poor biogas output. Because of the buffering capability of biochar, a more acceptable range for microbial activity was found. As a result, biochar plays a critical role in improving reactor stability by enhancing VFA decomposition in the digester.

3.2.3. Total and volatile solids change

AD is home to the essential intermediate products in the generation

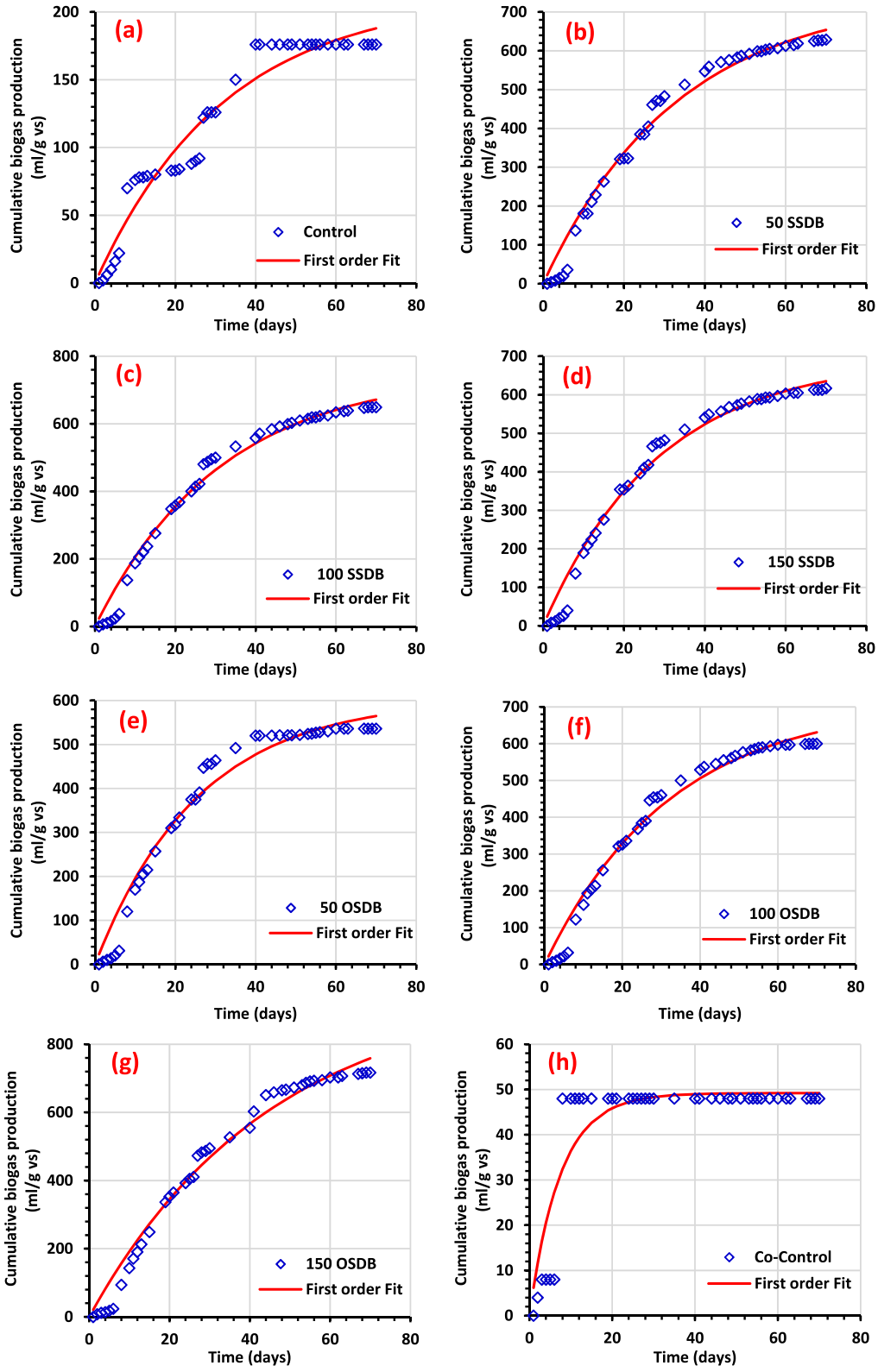

Fig. 11. The cumulative biogas yield calculated using a first-order model (a) Control (b-d) SSDB, (e-g) OSDB, (h) Co-Control (i-k) Co-SSDB and (L-n) Co-OSDB.

of biogas, which includes VS If the digester accumulates a significant amount of VS the digestion process may fail. As a result, the amount of VS is considered critical in determining the anaerobic reactor's operational state. When measuring the stability of the AD process, it is necessary to consider the deterioration of TS, and VS. Figs. 8 and 9 depict the TS trend during the e 70-day experiment. Throughout the digesting period, the TS content in all treatments decreased. Furthermore, the TS removal efficiencies ranged between 6.1 for 1 OSDB with

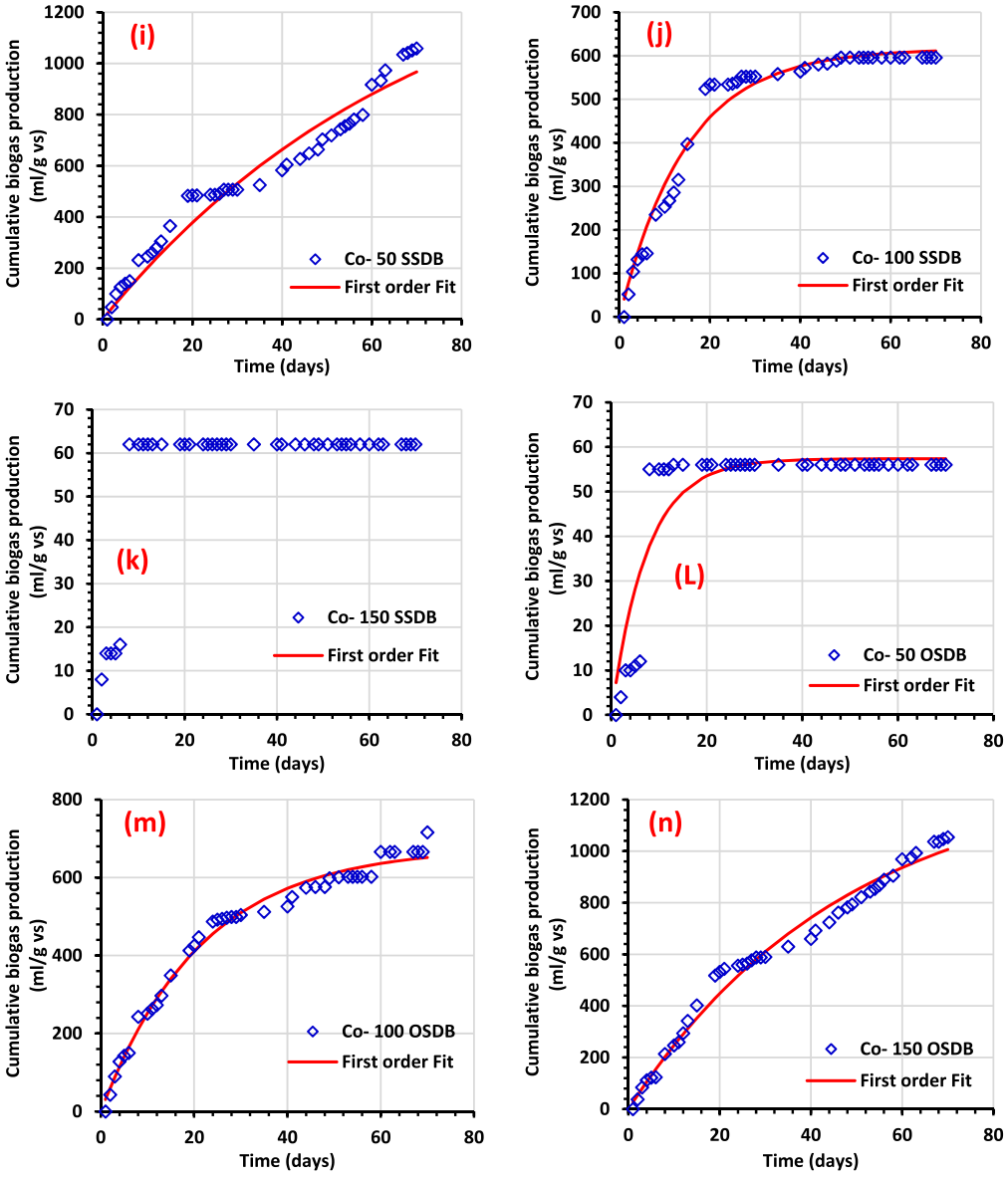

Fig. 11. (*continued*).

100 mg/L and 76.4 % for SSDB with 100 mg/L dosages, respectively. It's worth mentioning that in the case of Co of untreated algae with S. Parkle Co-control group, the digester accumulates a high amount of VS and leads to failure of the digestion processes, leading to a small amount of biogas production (48 mL/VS).

On the other hand, the VS removal efficiencies were 4 and 17.6 % for 100 mg/L of Co-SSDB and 100 mg/L of OSDB, respectively. Every bio-digester treatment tested decreased VS content throughout the trial. When different forms of biochar were added, the amount of organic matter degraded increased, which was indicated by changes in the total soluble solids and total volatile solids (TS and VS) content with each type of biochar added.

3.2.4. *Mechanism of US and O_3 effect on biochar properties*

Acoustic cavitation's chemical and mechanical properties are highly dependent on the US frequency [69]. Because of the increased jet velocity at low frequencies, the cavitation bubbles are more giant. Their collapses are more severe than at higher frequencies due to the more incredible jet velocity at low frequencies. Furthermore, it is generally established that shock waves heighten the physical effect of acoustic cavitation, shear stress, and jet flow, all of which are more abundant at low frequencies. Each of these variables contributes to the phenomenon. Additionally, Weiss [70] proposed that OH radicals would be generated during the breakdown of water, which was later confirmed by Makino et al. [71]. Under US, the generation of OH radicals happens both inside and around the interface between the cavity and the surrounding liquid during the hollow's collapse, allowing biochar's surface morphology and structural alteration to be altered in the presence of US (equations 12–14) [72]. (Fig. 5) indicates that the biogas production efficiency was enhanced by more than 3 folds when the carbon modified by US irradiation was used for the concentrations of 50, 100 and 150 mg/L for *C. Linum* only and increased by more than 6 folds when treated with Co-SSDB 50 mg/L. But it's also noticed that biogas production efficiency declined again as in sonicated SSDB 150 mg/L upon increasing the SD dosage. On the other hand, when the biochar was treated with O_3 dose 1.1 mg/L (Table 6), the massive increase in biogas production, specially the high dosage of OSDB 100 and 150 mg/L, unlike the US treatment, which favor the low dosage of OSDB 50 mg/L. Overall, the pH of the OSDB samples decreases dramatically, from neutral for the untreated OSDB to 1.87 ± 0.25 for the sample that was treated with O_3 for 30 min

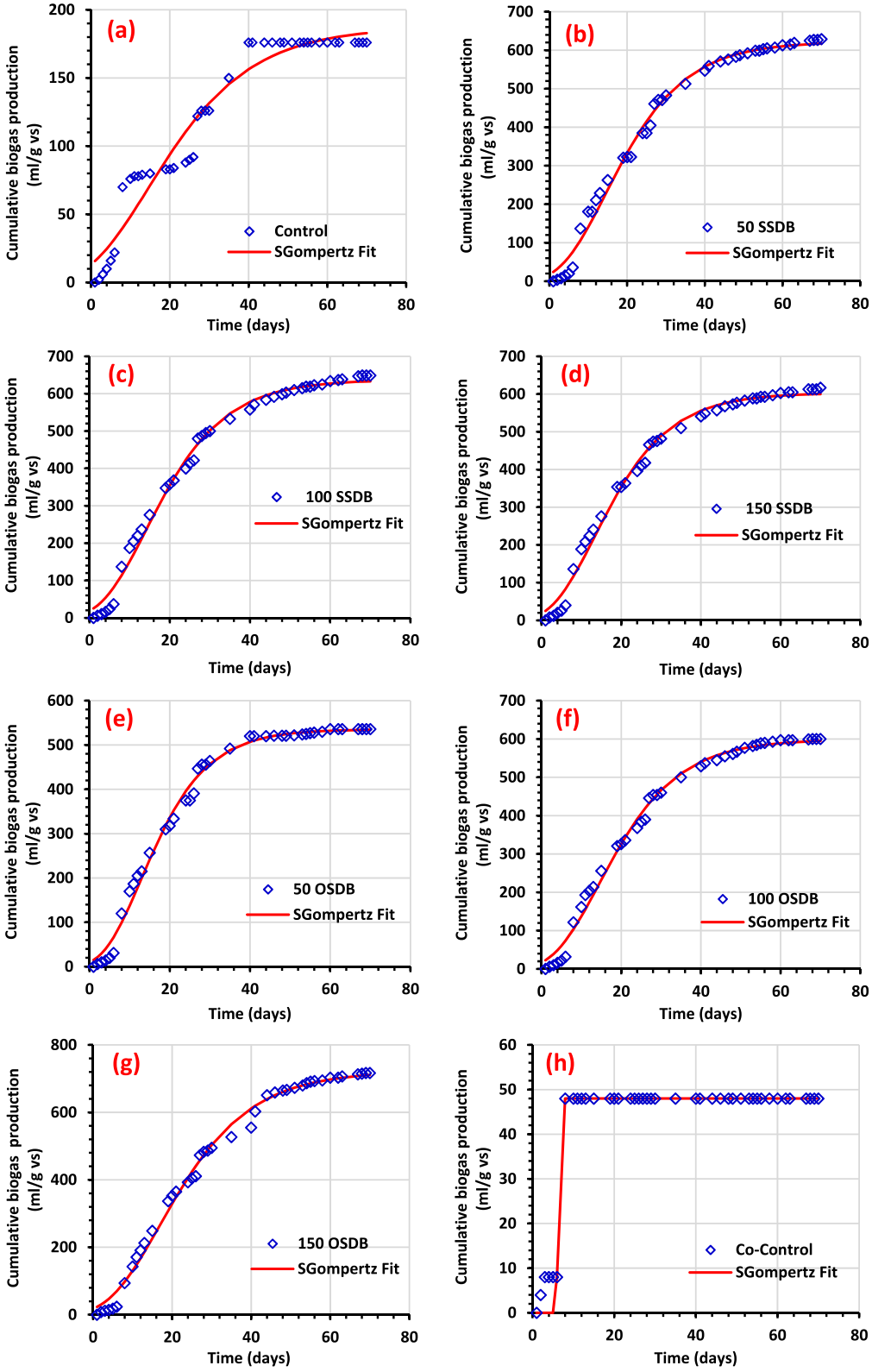

Fig. 12. The cumulative biogas yield calculated using the Gompertz model (a) Control (b-d) SSDB, (e-g) OSDB, (h) Co-Control (i-k) Co-SSDB and (L-n) Co-OSDB.

in all cases. In this case, it is thought that the addition of acidic oxygen-functional groups to the OSDB surface, particularly carboxyl groups, is the source of the dramatic pH drop that takes place very quickly. There is a relationship between treatment duration and increasing acidity in the OSDB samples, as evidenced by the pH trend. Due to the inhomogeneity and complexity of non OSDB material molecular structures, the reactions between it and oxygen can be quite complicated. According to the most likely scenario, the most significant interactions between O_3

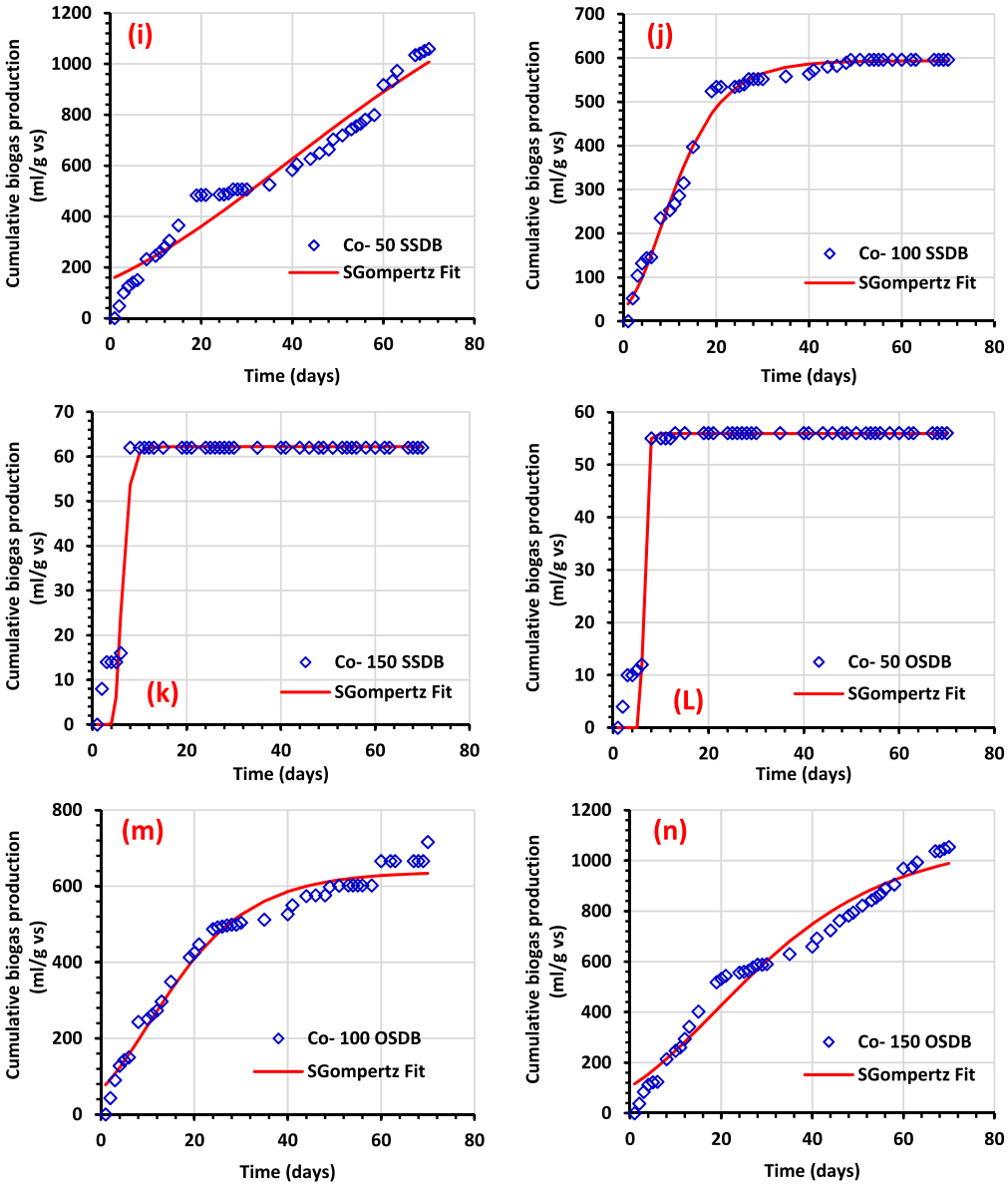

Fig. 12. (*continued*).

and organic matter involve the breakage of the carbon double bond, which acts as an excess electron nucleophile in these processes. For example, the injected O_3 air stream may, to a limited extent, contribute to the creation of carbonyl and carboxyl groups on OSDB surfaces by interacting with particular C═C double bonds in OSDB materials, as demonstrated in equations (20). The result will be an increase in the hydrophilicity of the ozonized OSDB product, which will be due to both the ability of the carbonyl and carboxyl groups to attract water molecules, as well as an increase in the cation exchange capacity (CEC) value, which will be due to the carboxyl groups readily deprotonating in water, resulting in a greater negative charge on the OSDB surfaces, as illustrated in equation (21). To characterize delocalized electrons, it has been discovered that the density of C═C structures is a useful metric [72–74]. Additional interactions with H_2O may be facilitated by the delocalized electron in SD, leading to the formation of the ions hydroxide (HO^-) and hydronium (H_3O^+) (Eq. (12)). In this case, through radical chain reactions, ^-OH could join with O_3 to produce a scavenger of reactive oxygen radicals (e.g., HO_2, O_2^-,·OH) in the presence of oxygen (Eqs. 15–19). As revealed by XRD characterisations, the presence of bicarbonate in SD, such as $CaCO_3$ or $MgCO_3$, may also contribute to ROS production during the O_3/SD process.

$$\text{Carbon-}\pi + H_2O \rightarrow \text{Carbon-}H_3O^+ + HO^- \quad (12)$$

$$H_2O \rightarrow HO^\bullet + H^\bullet \quad (13)$$

$$H^\bullet + O_2 \rightarrow HOO^\bullet \quad (14)$$

$$O_3 + HO^- \rightarrow H_2O^- + O_2 \quad (15)$$

$$O_3 + H_2O^- \rightarrow H_2O^\bullet + O_3^{\bullet-} \quad (16)$$

$$H_2O^\bullet \rightarrow O_3^{\bullet-} + H^+ \quad (17)$$

$$O_3^{\bullet-} \rightarrow O_2 + O^{\bullet-} \quad (18)$$

$$O^{\bullet-} + H_2O \rightarrow HO^\bullet + HO^- \quad (19)$$

$$\text{Biochars-CH} = \text{CH-Biochars} + O_3 \rightarrow \text{Biochars-COH} + \text{Biochars-COOH} \quad (20)$$

$$\text{Biochars-COOH} \rightarrow \text{Biochars-COO}^- + H^+ \quad (21)$$

3.3. Kinetics study

Detailed results of the kinetic investigation of natural gas production are shown in (Tables 7–9). The Gompertz and logistic feature models were found to be highly predictive of experimental results, with R^2 values greater than 0.94. For biogas generation using Co-OSDB (150 mg/L) and Co-SSDB (50 mg/L), Rm values of 25.66 and 38.49 mL/g VS were observed for the logistic model and modified Gompertz model (GM), respectively, for Co-OSDB (150 mg/L) and Co-SSDB (50 mg/L), for the logistic model and modified GM [38,53]. As predicted by the first-order model, the highest hydrolysis rates (K) were seen in the experiment with OSDB (50 mg/L) having 0.0.039 per day. Based on the data, the adjusted Gompertz and logistic models (GALM) have functional values of 0.02 and 0.07 days, respectively. Compared to the values published earlier for the modified GALM function [34,54], the value is exceedingly low in this work. As shown in (Figs. 10, 11, and 12), plotting the calculated values for biogas generation versus the observed values allows us to assess the model's trustworthiness in the context of the two models under consideration. (Tables 7 and 8) additionally give the statistical indicators (R^2), which provide context for the kinetics investigation. According to Nguyen et al. [38], better R^2 values (0.999 and 0.994, respectively) suggested a more appropriate kinetic model for the modified GALM feature. Both models have a higher R^2 of 0.992 than the other in our analysis.

4. Conclusions

When green algae *C. linum* is used as a substrate, conventional algal biomass's low carbon to nitrogen ratio might produce compounds detrimental to the digestive process, particularly ammonia. Reduced ammonia nitrogen concentrations can be achieved by combining algae with low-cost, high-carbon wastes, which may minimize ammonia inhibitor levels in the water. Because they served as bacteria colonies support, an electron transfer conductor between species, and a sorbent for indirect inhibitors or contaminants in *C. linum* and *S. parkle* fish food, the Co substrates were multifunctional in that they could promote biogas and biomethane production while also acting as an electron transfer conductor between species. A significant sorption ability to ammonium ions in both gaseous and aqueous form, pretreated biochar with US and O_3 can be used to reduce ammonium emissions from *N*-rich *S. parkles*. The greatest biogas yields were 1059 and 1054 mL/g, respectively, compared to SSDB's 50 mg/L and OSSDB's 150 mg/L. The results show that pretreatment biochar with US and O_3 removes inhibitors from the reaction medium throughout the AD process, improves the C/N ratio, and stabilizes anaerobic bacteria for biogas production. Future research should also examine the compatibility of the bioprocess, biogas emission, techno-economic analysis, and compositional analysis of the used seaweeds. According to our statistics, bioenergy is one of the main renewable energy sources that necessitate a generous financial investment. The worldwide, governments and societies should significantly contribute to developing more biogas and biomethane production facilities in the upcoming years to address the issue.

Funding

This study was not supported by any external funding.

CRediT authorship contribution statement

Ahmed El Nemr: Conceptualization, Methodology, Software, Supervision, Writing – review & editing. **Mohamed Aly Hassaan:** Conceptualization, Methodology, Software, Writing – original draft, Writing – review & editing. **Marwa Ramadan Elkatory:** Software, Writing – original draft. **Safaa Ragab:** Software. **Mohamed Ahmed El-Nemr:** Software. **Luigi Tedone:** . **Guisepe De Mastro:** . **Antonio Pantaleo:** .

Declaration of Competing Interest

The authors declare that they have no known competing financial interests or personal relationships that could have appeared to influence the work reported in this paper.

Data availability

Data will be made available on request.

References

[1] Y. Chen, J.J. Cheng, K.S. Creamer, Inhibition of anaerobic digestion process: a review, Bioresour. Technol. 99 (10) (2008) 4044–4064.
[2] C. Deng, R. Lin, X. Kang, B. Wu, R. O'Shea, J.D. Murphy, Improving gaseous biofuel yield from seaweed through a cascading circular bioenergy system integrating anaerobic digestion and pyrolysis, Renew. Sustain. Energy Rev. 128 (2020), 109895.
[3] F.C. Luz, S. Cordiner, A. Manni, V. Mulone, V. Rocco, R. Braglia, A. Canini, Ampelodesmos mauritanicus pyrolysis biochar in anaerobic digestion process: evaluation of the biogas yield, Energy 161 (2018) 663–669.
[4] N. Batta (2020). Bridging Thermochemical and Biochemical Conversion: Impact of Biochar Addition on the Anaerobic Digestion of Aqueous Pyrolysis Condensate. M. Sc Thesis, The University of Western Ontario, Canada.
[5] D. Fabbri, C. Torri, Linking pyrolysis and anaerobic digestion (Py-AD) for the conversion of lignocellulosic biomass, Curr. Opin. Biotechnol. 38 (2016) 167–173.
[6] S.R. Shanmugam, S. Adhikari, H. Nam, S.K. Sajib, Effect of bio-char on methane generation from glucose and aqueous phase of algae liquefaction using mixed anaerobic cultures, Biomass Bioenergy 108 (2018) 479–486.
[7] A. Anand, V. Kumar, P. Kaushal, Biochar and its twin benefits: Crop residue management and climate change mitigation in India, Renew. Sustain. Energy Rev. 156 (2022), 111959.
[8] F. Lü, C. Luo, L. Shao, P. He, Biochar alleviates combined stress of ammonium and acids by firstly enriching Methanosaeta and then Methanosarcina, Water Res. 90 (2016) 34–43.
[9] H. Zhou, R.C. Brown, Z. Wen, Biochar as an additive in anaerobic digestion of municipal sludge: Biochar properties and their effects on the digestion performance, ACS Sustainable Chem. Eng. 8 (16) (2020) 6391–6401.
[10] C. Torri, D. Fabbri, Biochar enables anaerobic digestion of aqueous phase from intermediate pyrolysis of biomass, Bioresour. Technol. 172 (2014) 335–341.
[11] M. Chen, D. Wang, F. Yang, X. Xu, N. Xu, X. Cao, Transport and retention of biochar nanoparticles in a paddy soil under environmentally-relevant solution chemistry conditions, Environ. Pollut. 230 (2017) 540–549.
[12] D. Wang, W. Zhang, X. Hao, D. Zhou, Transport of biochar particles in saturated granular media: effects of pyrolysis temperature and particle size, Environ. Sci. Technol. 47 (2) (2013) 821–828.
[13] G. Liu, H. Zheng, Z. Jiang, J. Zhao, Z. Wang, B. Pan, B. Xing, Formation and physicochemical characteristics of nano biochar: insight into chemical and colloidal stability, Environ. Sci. Technol. 52 (18) (2018) 10369–10379.
[14] S. Chen, J. Zhang, X. Wang, Effects of alkalinity sources on the stability of anaerobic digestion from food waste, Waste Manage. Res. 33 (11) (2015) 1033–1040.
[15] M. Mun, H. Cho, Mineral carbonation for carbon sequestration with industrial waste, Energy Procedia 37 (2013) 6999–7005.
[16] M. Zhang, J. Li, Y. Wang, C. Yang, Impacts of different biochar types on the anaerobic digestion of sewage sludge, RSC Adv. 9 (72) (2019) 42375–42386.
[17] M.A. Hassaan, A. El Nemr, M.R. Elkatory, S. Ragab, M.A. El-Nemr, A. Pantaleo, Synthesis, characterization, and synergistic effects of modified biochar in combination with α-Fe_2O_3 NPs on biogas production from red algae Pterocladia capillacea, Sustainability 13 (16) (2021) 9275.
[18] A. El Nemr, M.A. Hassaan, M.R. Elkatory, S. Ragab, A. Pantaleo, Efficiency of Fe_3O_4. Nanoparticles with different pretreatments for enhancing biogas yield of macroalgae *Ulva intestinalis* Linnaeus, Molecules 26 (16) (2021) 5105.
[19] M.A. El-Nemr, N.M. Abdelmonem, I. Ismail, S. Ragab, A. El Nemr, Ozone and ammonium hydroxide modification of biochar prepared from *Pisum sativum* peels improves the adsorption of copper (II) from an aqueous medium, Environ. Processes 7 (3) (2020) 973–1007.
[20] M.A. El-Nemr, N.M. Abdelmonem, I.M. Ismail, S. Ragab, A. El Nemr, The efficient removal of the hazardous Azo Dye Acid Orange 7 from water using modified biochar from Pea peels, Desalin. Water Treat. 203 (2020) 327–355.
[21] M.A. El-Nemr, N.M. Abdelmonem, I.M. Ismail, S. Ragab, A. El Nemr, Removal of acid yellow 11 dye using novel modified biochar derived from watermelon peels, Desalin. Water Treat. 203 (2020) 403–431.
[22] R. Chatterjee, B. Sajjadi, D.L. Mattern, W.Y. Chen, T. Zubatiuk, D. Leszczynska, J. Leszczynski, N.O. Egiebor, N. Hammer, Ultrasound cavitation intensified amine functionalization: a feasible strategy for enhancing CO_2 capture capacity of biochar, Fuel 225 (2018) 287–298.
[23] T. Lippert, J. Bandelin, D. Vogl, Z. Alipour Tesieh, T. Wild, J.E. Drewes, K. Koch, Full-scale assessment of ultrasonic sewage sludge pretreatment using a novel double-tube reactor, ACS ES&T Eng. 1 (2) (2020) 298–309.
[24] C. Bougrier, H. Carrère, J.P. Delgenes, Solubilisation of waste-activated sludge by ultrasonic treatment, Chem. Eng. J. 106 (2) (2005) 163–169.

[25] A. Tiehm, K. Nickel, M. Zellhorn, U. Neis, Ultrasonic waste activated sludge degradation for improving anaerobic stabilization, Water Resour. 35 (8) (2001) 2003–2009.
[26] U. Neis, K. Nickel, A. Tiehm, Enhancement of anaerobic sludge digestion by ultrasonic disintegration, Water Sci. Tech. 42 (9) (2000) 73–80.
[27] M.A. Hassaan, A. El Nemr, F.F. Madkour, Testing the advanced oxidation processes on the degradation of Direct Blue 86 dye in wastewater, Egypt. J. Aquat. Res. 43 (1) (2017) 11–19.
[28] A. El Nemr, M.A. Hassaan, F.F. Madkour, Advanced oxidation process (AOP) for detoxification of acid red 17 dye solution and degradation mechanism, Environ. Processes. 5 (1) (2018) 95–113.
[29] A.E. Greenberg, Standard methods for the examination of water and wastewater, Am. Public. Health Association (1980) 409–426.
[30] K. Rakness, G. Gordon, B. Langlais, W. Masschelein, N. Matsumoto, Y. Richard, C. M. Robson, I. Somiya, Guideline for measurement of ozone concentration in the process gas from an ozone generator, Ozone Sci. Eng. 18 (3) (1996) 209–229.
[31] M.F. Kamaroddin, J. Hanotu, D.J. Gilmour, W.B. Zimmerman, In-situ disinfection and a new downstream processing scheme from algal harvesting to lipid extraction using ozone-rich microbubbles for biofuel production, Algal Res. 17 (2016) 217–226.
[32] M.D. Huff, S. Marshall, H.A. Saeed, J.W. Lee, Surface oxygenation of biochar through ozonization for dramatically enhancing cation exchange capacity, Bioresour. Bioprocess. 5 (1) (2018) 1–9.
[33] A. Ali, R.B. Mahar, E.M. Abdelsalam, S.T. Sherazi, Kinetic modeling for bioaugmented anaerobic digestion of the organic fraction of municipal solid waste by using Fe_3O_4 nanoparticles, Waste Biomass Valorization 10 (11) (2019) 3213–3224.
[34] D.D. Nguyen, B.H. Jeon, J.H. Jeung, E.R. Rene, J.R. Banu, B. Ravindran, C.M. Vu, H.H. Ngo, W. Guo, S.W. Chang, Thermophilic anaerobic digestion of model organic wastes: Evaluation of biomethane production and multiple kinetic models analysis, Bioresour. Technol. 280 (2019) 269–276.
[35] G.K. Kafle, L. Chen, Comparison on batch anaerobic digestion of five different livestock manures and prediction of biochemical methane potential (BMP) using different statistical models, Waste Manage. 48 (2016) 492–502.
[36] A. Donoso-Bravo, S.I. Pérez-Elvira, F. Fdz-Polanco, Application of simplified models for anaerobic biodegradability tests. Evaluation of pre-treatment processes, Chem. Eng. J. 160 (2) (2010) 607–614.
[37] M. Stefaniuk, P. Oleszczuk, Characterization of biochars produced from residues from biogas production, J. Anal. Appl. Pyrolysis. 115 (2015) 157–165.
[38] S. Alghashm, S. Qian, Y. Hua, J. Wu, H. Zhang, W. Chen, G. Shen, Properties of biochar from anaerobically digested food waste and its potential use in phosphorus recovery and soil amendment, Sustainability. 10 (12) (2018) 4692.
[39] C.E. Brewer, K. Schmidt-Rohr, J.A. Satrio, R.C. Brown, Characterization of biochar from fast pyrolysis and gasification systems, Environ. Prog. Sustainable Energy 28 (3) (2009) 386–396.
[40] S.A. Opatokun, T. Kan, A. Al Shoaibi, C. Srinivasakannan, V. Strezov, Characterization of food waste and its digestate as feedstock for thermochemical processing, Energy Fuels 30 (3) (2016) 1589–1597.
[41] K.H. Kim, J.Y. Kim, T.S. Cho, J.W. Choi, Influence of pyrolysis temperature on physicochemical properties of biochar obtained from the fast pyrolysis of pitch pine (Pinus rigida), Bioresour. Technol. 118 (2012) 158–162.
[42] R. Samson, A. LeDuy, Improved performance of anaerobic digestion ofSpirulina maxima algal biomass by addition of carbon-rich wastes, Biotechnol. Lett. 5 (10) (1983) 677–682.
[43] H.W. Yen, D.E. Brune, Anaerobic co-digestion of algal sludge and waste paper to produce methane, Bioresour. Technol. 98 (1) (2007) 130–134.
[44] S. Kloss, F. Zehetner, A. Dellantonio, R. Hamid, F. Ottner, V. Liedtke, M. Schwanninger, M.H. Gerzabek, G. Soja, Characterization of slow pyrolysis biochars: effects of feedstocks and pyrolysis temperature on biochar properties, J. Environ. Qual. 41 (4) (2012) 990–1000.
[45] S.M. Taha, M.E. Amer, A.E. Elmarsafy, M.Y. Elkady, Adsorption of 15 different pesticides on untreated and phosphoric acid treated biochar and charcoal from water, J. Environ. Chem. Eng. 2 (4) (2014) 2013–2025.
[46] D.C. Tsang, J. Hu, M.Y. Liu, W. Zhang, K.C. Lai, I. Lo, Activated carbon produced from waste wood pallets: adsorption of three classes of dyes, Water Air Soil Pollut. 184 (1) (2007) 141–155.
[47] B. Sajjadi, J.W. Broome, W.Y. Chen, D.L. Mattern, N.O. Egiebor, N. Hammer, C. L. Smith, Urea functionalization of ultrasound-treated biochar: A feasible strategy for enhancing heavy metal adsorption capacity, Ultrason. Sonochem. 51 (2019) 20–30.
[48] M. Myglovets, O.I. Poddubnaya, O. Sevastyanova, M.E. Lindström, B. Gawdzik, M. Sobiesiak, M.M. Tsyba, V.I. Sapsay, D.O. Klymchuk, A.M. Puziy, Preparation of carbon adsorbents from lignosulfonate by phosphoric acid activation for the adsorption of metal ions, Carbon 80 (2014) 771–783.
[49] R. Watanabe, C. Tada, Y. Baba, Y. Fukuda, Y. Nakai, Enhancing methane production during the anaerobic digestion of crude glycerol using Japanese cedar charcoal, Bioresour. Technol. 150 (2013) 387–392.
[50] J. Pan, J. Ma, X. Liu, L. Zhai, X. Ouyang, H. Liu, Effects of different types of biochar on the anaerobic digestion of chicken manure, Bioresour. Technol. 275 (2019) 258–265.
[51] A.D. Junior, C. Etchebehere, D. Perecin, S. Teixeira, J. Woods, Advancing anaerobic digestion of sugarcane vinasse: Current development, struggles and future trends on production and end-uses of biogas in Brazil, Renew. Sustain. Energy Rev. 157 (2022), 112045.
[52] K.T. Dasa, S.Y. Westman, R. Millati, M.N. Cahyanto, M.J. Taherzadeh, C. Niklasson, Inhibitory effect of long-chain fatty acids on biogas production and the protective effect of membrane bioreactor, Biomed Res. Int. (2016), https://doi.org/10.1155/2016/7263974.
[53] K. Hanaki, T. Matsuo, M. Nagase, Mechanism of inhibition caused by long-chain fatty acids in anaerobic digestion process, Biotechnol. Bioeng. 23 (7) (1981) 1591–1610.
[54] O. Stabnikova, S.S. Ang, X.Y. Liu, V. Ivanov, J.H. Tay, J.Y. Wang, The use of hybrid anaerobic solid–liquid (HASL) system for the treatment of lipid-containing food waste, J. Chem. Technol. Biotechnol.: Int. Res. Process Environ. Clean Technol. 80 (4) (2005) 455–461.
[55] L.J. Wu, T. Kobayashi, Y.Y. Li, K.Q. Xu, Comparison of single-stage and temperature-phased two-stage anaerobic digestion of oily food waste, Energy Convers. Manage. 106 (2015) 1174–1182.
[56] I.W. Koster, A. Cramer, Inhibition of methanogenesis from acetate in granular sludge by long-chain fatty acids, Appl. Environ. Microbiol. 53 (2) (1987) 403–409.
[57] A. Rinzema, M. Boone, K. van Knippenberg, G. Lettinga, Bactericidal effect of long chain fatty acids in anaerobic digestion, Water Environ. Res. 66 (1) (1994) 40–49.
[58] E. Kovács, R. Wirth, G. Maróti, Z. Bagi, G. Rákhely, K.L. Kovács, Biogas production from protein-rich biomass: fed-batch anaerobic fermentation of casein and of pig blood and associated changes in microbial community composition, PLoS ONE 8 (10) (2013) e77265.
[59] K.V. Rajeshwari, M. Balakrishnan, A. Kansal, K. Lata, V.V. Kishore, State-of-the-art of anaerobic digestion technology for industrial wastewater treatment, Renew. Sustain. Energy Rev. 4 (2) (2000) 135–156.
[60] B. Demirel, O. Yenigun, Two-phase anaerobic digestion processes: a review, J. Chem. Technol. Biotechnol. 77 (2002) 743–755.
[61] S. Luste, S. Luostarinen, Anaerobic co-digestion of meat-processing by-products and sewage sludge–effect of hygienization and organic loading rate, Bioresour. Technol. 101 (8) (2010) 2657–2664.
[62] Z. Wu, X. Chen, S. Zhu, Z. Zhou, Y. Yao, W. Quan, B. Liu, Enhanced sensitivity of ammonia sensor using graphene/polyaniline nanocomposite, Sens. Actuators, B 178 (2013) 485–493.
[63] M. Yao, Y.C. Woo, J. Ren, L.D. Tijing, J.S. Choi, S.H. Kim, H.K. Shon, Volatile fatty acids and biogas recovery using thermophilic anaerobic membrane distillation bioreactor for wastewater reclamation, J. Environ. Manage. 231 (2019) 833–842.
[64] N.M. Saady, D.I. Massé, Impact of organic loading rate on the performance of psychrophilic dry anaerobic digestion of dairy manure and wheat straw: long-term operation, Bioresour. Technol. 182 (2015) 50–57.
[65] E. Kwietniewska, J. Tys, Process characteristics, inhibition factors and methane yields of anaerobic digestion process, with particular focus on microalgal biomass fermentation, Renew. Sustain. Energy Rev. 34 (2014) 491–500.
[66] A.J. Ward, P.J. Hobbs, P.J. Holliman, D.L. Jones, Optimisation of the anaerobic digestion of agricultural resources, Bioresour. Technol. 99 (17) (2008) 7928–7940.
[67] G. Esposito, L. Frunzo, A. Giordano, F. Liotta, A. Panico, F. Pirozzi, Anaerobic co-digestion of organic wastes, Rev. Environ. Sci. Bio/Technol. 11 (4) (2012) 325–341.
[68] B. Molinuevo-Salces, M.C. García-González, C. González-Fernández, M.J. Cuetos, A. Morán, X. Gómez, Anaerobic co-digestion of livestock wastes with vegetable processing wastes: a statistical analysis, Bioresour. Technol. 101 (24) (2010) 9479–9485.
[69] M.L. Garcia, L.T. Angenent, Interaction between temperature and ammonia in mesophilic digesters for animal waste treatment, Water Res. 43 (9) (2009) 2373–2382.
[70] J. Weiss, Radiochemistry of aqueous solutions, Nature 153 (3894) (1944) 748–7450.
[71] K. Makino, M.M. Mossoba, P. Riesz, Chemical effects of ultrasound on aqueous solutions. Evidence for hydroxyl and hydrogen free radicals (cntdot. OH and. cntdot. H) by spin trapping, J. Am. Chem. Soc. 104 (12) (1982) 3537–3539.
[72] H. Li, S. Liu, S. Qiu, L. Sun, X. Yuan, D. Xia, Catalytic ozonation oxidation of ketoprofen by peanut shell-based biochar: effects of the pyrolysis temperatures, Environ. Technol. 20 (2020) 1–3.
[73] N. Leconte, J. Moser, P. Ordejon, H. Tao, A. Lherbier, A. Bachtold, F. Alsina, C. M. Sotomayor Torres, J.C. Charlier, S. Roche, Damaging graphene with ozone treatment: a chemically tunable metal– insulator transition, ACS Nano 4 (7) (2010) 4033–4038.
[74] J. Rivera-Utrilla, M. Sánchez-Polo, Ozonation of 1, 3, 6-naphthalenetrisulphonic acid catalysed by activated carbon in aqueous phase, Appl. Catal. B 39 (4) (2002) 319–329.